**TRIBHUVAN UNIVERSITY**
**INSTITUTE OF ENGINEERING**
**PULCHOWK CAMPUS**
**DEPARTMENT OF CIVIL ENGINEERING**

# FINAL YEAR PROJECT REPORT ON STUDY OF COMBINED PILE RAFT FOUNDATION ON THE SOIL OF CHAKUPAT AREA

By:

Aastha Pathak (075BCE006)
Anil Mahat (075BCE019)
Bikram Paudel (075BCE038)
Binayaraj Shrestha (075BCE039)
Binit Banstola (075BCE040)
Bipin Chhantyal (075BCE042)

Supervisor:

Asst. Prof. Bhim Kumar Dahal, Ph.D.
Department of Civil Engineering

**BAISHAKH 2080**

**TRIBHUVAN UNIVERSITY**
**INSTITUTE OF ENGINEERING**
**PULCHOWK CAMPUS**
**DEPARTMENT OF CIVIL ENGINEERING**

# FINAL YEAR PROJECT REPORT ON
# STUDY OF COMBINED PILE RAFT FOUNDATION ON THE SOIL OF CHAKUPAT AREA

*In Partial Fulfilment of The Requirement for The Award of Bachelor Degree in Civil Engineering*
**(Course Code: CE755)**

By:

Aastha Pathak (075BCE006)
Anil Mahat (075BCE019)
Bikram Paudel (075BCE038)
Binayaraj Shrestha (075BCE039)
Binit Banstola (075BCE040)
Bipin Chhantyal (075BCE042)

Supervisor:

Asst. Prof. Bhim Kumar Dahal, Ph.D.
Department of Civil Engineering

**BAISHAKH 2080**

# COPYRIGHT



Head of Department
Department of Civil Engineering
Pulchowk Campus
Institute of Engineering
Lalitpur, Nepal

**TRIBHUVAN UNIVERSITY**
**INSTITUTE OF ENGINEERING**
**PULCHOWK CAMPUS**
**DEPARTMENT OF CIVIL ENGINEERING**

# CERTIFICATE

This is to certify that this project work entitled "STUDY OF COMBINED PILE RAFT FOUNDATION ON THE SOIL OF CHAKUPAT AREA" submitted by Aastha Pathak, Anil Mahat, Bikram Paudel, Binayaraj Shrestha, Binit Banstola and Bipin Chhantyal has been examined and declared successful for the fulfilment of academic requirement towards the completion of Bachelor Degree in Civil Engineering

.....
Asst. Prof. Dr. Bhim K Dahal
Project Supervisor

.....
Prof. Dr. Gokarna B. Motra
HOD, Department of Civil Engineering

.....
Dr. Indra P. Acharya
External Examiner

.....
Gopal Singh Bhandari
Internal Examiner

# ABSTRACT

Traditional foundations cannot support a structure on weak soil or heavily settling soil. For the purpose of controlling settlement, pile raft foundations are used, with the raft part providing additional capacity at ultimate loading while the piles provide the majority of stiffness under serviceability loads. The utilisation of pile raft foundations in the Chakupat area which lies in the Kathmandu Valley is the subject of this research. The Kathmandu Valley is located in an earthquake-prone area. After the 2015 earthquake, it is suggested to implement a more solid and appropriate building strategy. The ideal alternative for the construction is a piling raft foundation. As more and more tall structures are constructed in Kathmandu, the pile raft foundation has a good chance of success in the valley of Kathmandu.

This research explains the idea behind using piles to reduce settlement for raft foundations as well as how pile rafts behave in the soil of Chakupath area. Model tests using the ideas of an embedded pile and a volumetric pile are carried out and compared.This study shows the percentage of weight carried by piles in the CPRF (Combined pile raft foundation) falls as the number of piles is reduced, and increases as pile length is raised. The findings of the model were compared with other papers as well as with analytical calculations for confirmations. A foundation with raft thickness of 0.6 m, pile length of 15 m, diameter of 1 m, and spacing of 4 m is the most suited in Chakupat Area when taking into consideration the examination of the soil structure, settlement, economy, and load sharing. The results show that the CPRF model has a bearing capacity of 573969.62kN, a factor of safety of 4.42, and a stiffness of 433886.01 kN/m.

The estimated cost for the selected model was NRs. 76109910.25. The study concluded that CPRF was a feasible foundation for the soil of the Chakupat area, and the proposed model was safe for construction. The findings can provide valuable information for future construction projects in the area, and the cost estimation can aid in budget planning.

Keywords: Kathmandu Valley, Chakupat Area, Pile raft foundation, Finite analysis, Plaxis 3D, CPRF,, Settlement, Stiffness, Earthquake-prone area, Embedded pile, Volumetric pile, Bearing capacity, Factor of safety, Soil structure, Load sharing, Economy, Cost estimation, Construction.

# ACKNOWLEDGEMENT

The completion of this project has been made possible through continuous support of our respected teachers, seniors, friends and well-wishers. We would like to express our most sincere gratitude to Associate Professor Dr. Bhim Kumar Dahal for continuously supporting and supervising us throughout the process. We are also equally indebted to him for providing us with the required data for the project. We are humbled for the trust and confidence; he has shown to us.

We would also like to express our thanks towards Associate Professor Kalyan Poudel, for providing guidance whenever needed. His support for this endeavour cannot be understated. Also we would like to thank Technical Officer Rajendra Panta for guiding us in our lab work. We also like to thank our family members who were the helping hands during this project.

Finally, we would like to thank IOE for providing us such an opportunity to perform this project as a part of the final year project.

Aastha Pathak 075BCE006

Anil Mahat 075BCE019

Bikram Paudel 075BCE038

Binayaraj Shrestha 075BCE039

Binit Banstola 075BCE040

Bipin Chhantyal 075BCE042

# TABLE OF CONTENTS

# LIST OF FIGURES

# LIST OF TABLES

# NOTATIONS

| | |
|---|---|
| C | Cohesion of soil |
| e | Eccentricity |
| E | Modulus of elasticity |
| G | Shear modulus of elasticity |
| K | Stiffness |
| M | Bending Moment |
| q | Overburden pressure |
| Q | Imposed vertical load |
| R | Resistance |
| Se | Elastic settlement |
| Φ | Internal friction angle of the soil |
| γ | Unit Weight of Soil |
| $\alpha_{rp}$ | Raft pile interaction factor |
| $\alpha_{pp}$ | Pile to pile interaction factor |
| $\alpha_{pr}$ | Pile raft interaction factor |
| η | CPRF efficiency factor |
| ρ | Soil variable stiffness |
| ν | Poisson ratio |
| $w_t$ | Settlement of pile head |
| $K_g$ | Stiffness of group pile |
| $K_r$ | Stiffness of raft |
| Kpr | Stiffness of combined pile raft foundation |
| Esav | Average Young's modulus of soil along pile shaft |

$\rho$ Variation of soil modulus with depth

$E_{sl}$ Young's modulus of soil at level of pile tip

$E_{sb}$ Young's Modulus of soil at bearing stratum below pile

# ABBREVIATIONS

| | |
|---|---|
| IS | Indian Standard |
| BS | British Standard |
| AS | American Standard |
| CPRF | Combined Pile Raft Foundation |
| FEM | Finite Element Method |
| SPT | Standard Penetration Test |
| CPT | Cone Penetration Test |
| FOS | Factor of safety |
| PI | Plasticity Index |
| PL | Plastic Limit |
| LL | Liquid Limit |
| ISO | International Organization for Standardization |
| IOE | Institute of Engineering |
| TU | Tribhuvan University |
| 2D | Two Dimensional |
| 3D | Three Dimensional |

# Chapter 1: Introduction

## 1.1 Background of study

Kathmandu Valley, located in the central part of Nepal, is a unique geological feature formed by the convergence of two major tectonic plates: the Indian Plate and the Eurasian Plate. The valley is a graben, which means that it is a depressed block of land that is surrounded by parallel faults.

The geology of the Kathmandu Valley is dominated by sediments, which are deposits of rocks, minerals, and organic matter that have been transported and deposited by water, wind, or ice. These sediments are composed of a wide variety of materials, including sand, gravel, silt, and clay.

The valley is also characterised by its alluvial fan deposits, which are deposits of sediment that have been carried by streams and rivers and deposited on the valley floor. These alluvial fan deposits are composed of fine-grained sediments, such as silt and clay, as well as coarser sediments, such as sand and gravel.

Building practices in Kathmandu Valley involve traditional materials such as brick, mud, and timber, and are characterised by intricate carvings and ornamental details. Modern practices such as reinforced concrete and steel have become more common, leading to concerns over seismic safety and preservation of traditional architecture. The government has implemented building codes and regulations, but enforcement is inconsistent, leaving many older buildings vulnerable to seismic activity. Continued efforts are needed to balance preservation with safety concerns.

Kathmandu Valley has a unique geology, and the type of foundation used for buildings depends on several factors, including the soil type, groundwater level, and seismic activity. Here are some of the common types of foundation used in the Kathmandu Valley:

1. Spread Footing: This type of foundation is used when the soil is stable and can support the weight of the building. Spread footings distribute the load of the building over a wide area and are suitable for low-rise structures.

2. Raft Foundation: Raft foundations are used when the soil is weak, and the load-bearing capacity is limited. They are suitable for multi-story buildings and transfer the weight of the structure over a larger area.

3. Pile Foundation: Pile foundations are used when the soil is not suitable for spread footings or raft foundations. Pile foundations transfer the weight of the structure to a deeper layer of stable soil or rock.

4. Caisson Foundation: Caisson foundations are similar to pile foundations, but instead of using individual piles, they use a large concrete column or pier that is sunk into the ground.

5. Stone and Masonry Foundation: Stone and masonry foundations are commonly used in traditional Nepalese buildings. The foundation is made of large stones or bricks that are laid on top of each other without mortar. The weight of the building compresses the stones and creates a stable foundation.

In the case of tall or heavy structures, traditional shallow foundations may not be adequate, and deep foundations such as pile foundations are required. However, pile foundations can be expensive and time-consuming to construct, which has led to the development of combined pile raft foundations.

A combined pile raft foundation is a foundation that merges the advantages of both pile and raft foundations. It utilizes piles to transmit the load of the structure to deeper, more stable soil layers, while the raft foundation provides a broad base area to spread the load evenly. It is commonly used for large structures such as tall buildings and bridges.

Despite its numerous advantages, the design of combined pile raft foundations still requires analysis and optimization. In order to ensure stability and safety, it is essential to have a comprehensive understanding of the foundation's behavior under different soil types and loading conditions. As a result, the analysis of combined pile raft foundations has received significant attention in recent years.

This research intends to enhance the understanding of combined pile raft foundations by analysing their behaviour under various conditions. The study's goal is to provide insight into the optimization of combined pile raft foundation design and ensure its stability and safety by exploring the performance of this type of foundation.

## 1.2 Objectives

1. Improved understanding: One of the primary objectives of research and analysis on CPRF is to improve the understanding of the behaviour and performance of this foundation system. This includes understanding how the combination of piles and a raft foundation affects the load-bearing capacity, settlement, and resistance to lateral forces of the foundation.

2. Optimization: This includes identifying the most effective pile spacing, pile length, pile diameter, and raft thickness for a given building and soil condition.(main objective and analysis done in the project.)

3. Bearing capacity and settlement: To calculate the bearing capacity and settlement of CPRF on the proposed soil specifications for given building load.

4. Load distribution: For calculation of load distribution among pile and raft and finding load distribution ratio.

### 1.3 Scope of the study

The scope of the study or work that will be explored on CPRF includes:

1. Investigating the behaviour of CPRF under different loading and soil conditions.

2. Studying the soil parameters of the given place and model the CPRF for a loading system over it.

3. Analysing the performance of CPRF compared to other foundation systems.

4. Determine the load distribution in pile and raft as well as evaluation of the settlement of both pile and raft.

5. Verifying the estimated outputs analytically.

6. Checking the validity of the output referring to the prevalent design codes and literatures.

7. Making recommendations for the design and construction of CPRF.

### 1.4 Importance of CPRF

On why CPRF is important and why is it worth studying or using are explained below:

1. Improved load-bearing capacity: CPRF has the ability to support higher loads than other foundation systems, making it suitable for tall and heavy structures.

2. Reduced settlement: CPRF can reduce settlement compared to other foundation types, which is particularly important in areas with poor soil conditions.

3. Resistance to lateral forces: CPRF provides better resistance to lateral forces such as wind and earthquakes, which can improve the safety of the building.

4. Cost-effective: CPRF can be more cost-effective than other foundation systems, particularly in situations where there are poor soil conditions and a large number of piles are required.

5. Sustainability: CPRF can be designed and constructed using sustainable materials, reducing the environmental impact of the construction process.

Overall, CPRF is an important foundation system that can provide improved load-bearing capacity, reduced settlement, resistance to lateral forces, cost-effectiveness, and sustainability. As such, it is worth studying and considering for use in appropriate building projects.

### 1.5 Structure of the report

**Chapter one** gives an introduction of CPRF, design approach, objectives, scope of study and importance of studying and considering the use of CPRF in different building projects.

**Chapter two** offers a thorough review of existing literature regarding the bearing capacity and settlement of CPRF, as well as various analytical and design methods used for this type of foundation.

**Chapter three** outlines the methodology and approach taken to analyse CPRF, with flowchart.

**Chapter four** represents the result of models of CPRF from PLAXIS 3D and analytical formulas, the validation of the project via prevailing building codes and literature reviews and findings.

**Chapter five** offers design of suitable models.

**Chapter six** presents the conclusion of the study and recommendations for further possible improvements that can be done.

**Appendix A** gives soil parameters from the laboratory.

**Appendix B** presents classification of soil.

**Appendix C** gives analytical calculations for design and validation of CPRF.

**Appendix D** represents table of bearing capacity factors.

**Appendix E** shows relation between poisson's ratio and liquid limit of soil.

**Appendix F** shows pile location table.

**Appendix G** shows calculation results of the plate.

**Appendix H** shows calculation results of embedded beams.

**Appendix I** shows general quantity estimation.

## Chapter 2: Literature review

It is common practice in foundation design to first consider employing a shallow foundation system, similar to a raft, to support a structure. If this is insufficient, however, a fully piled foundation is designed, where the piles are responsible for withstanding all of the design loads. The pile raft foundation, also known as a raft foundation improved with deep foundations, has drawn a lot of attention lately.

Different technical reports for settlement prediction on pile raft has been prepared. Different approaches have been made to design the pile raft foundations. Randolph (1994) provided proposals for creating piled raft foundations, giving settlement more focus than load bearing capacity, and offered design techniques for calculating the number of piles needed in CPRF to reduce settlement. Poulos (2001) used mathcad analysis to obtain the settlement along with the computer programs GARP and DEFPIG. Prakoso and Kulhawy (2001) used linear elastic and non-linear plane strain finite element methods using PLAXIS.According to Kim et al. (2001), the soil and piles are recreated as Winkler and linked springs, respectively, and the raft appears as a plate based on the Mindlin theory. The approximate analytical method put out by Randolph and Wroth is used to determine the stiffness of piles, and the subgrade reaction's modulus is used to get the Winkler spring constant.Kitiyodom and Matsumoto (2003) used simplified method of numerical analysis to analyse axially and laterally loaded piled raft foundations embedded in non-homogenous soil by computer program called PRAB. In order to analyze the lateral response of the foundation, Poulos and Chow (2011) used a proprietary program named CLAP (Combined Load Analysis of Piles) as the primary design tool. Srilakshmi and Moudgalya(2013) analysed pile raft foundation in medium sand using parametric study and finite analysis using software ANSYS.Unsever and Matsumoto (2015) modeled sand using a hardening soil model, while the pile and raft were modeled using an elastic model in PLAXIS. Tradigo et al.(2016) used both embedded pile concept and fully solid concept to numerically analyse disconnected pile and raft. Deb and Pal (2019) used 3d finite element analysis for load sharing response model. Azhar et al. (2020) used parametric study for deciding the suitable configuration of the piled raft foundation and designing it.

There are three steps in the design process for a piled raft. An initial, preliminary step involves performing an approximation of the effects of the number of piles on load capacity and settling. The second is an in-depth investigation to identify the locations where piles are required as well as to acquire a broad notion of the piling requirements. The third stage is the detailed design phase, where a more extensive investigation is utilized to verify the optimal number and positioning of the piles as

well as to obtain essential information for the structural design of the foundation system. (Polous , 2001).

Prakoso and Kulhawy (2001) studied the behaviour of vertically loaded piled rafts using elastic and elastic-plastic plane strain finite element methods. He found that the pile group to raft width ratio and the pile depth have the most effects on the system geometry. While a width ratio of approximately 0.5 is most useful for minimizing differential movement, a width ratio of 1 is effective for minimizing average displacement.

The fundamentals of a limit state design approach were established by Poulos and Chow (2011) for built raft foundations for tall buildings. These conditions include cyclic loading, serviceability, and ultimate limit states. Both small and full-scale models (the Incheon tower) have been created. The calculations for the small-scale test showed that the effect of the soil on the buried cap was significant and led to an overestimation of the lateral deflection and an underestimate of the lateral load capacity. Additionally, the full scale finite analysis recommended that, when the basement effect was taken into account, lateral deflections would be less than those of a raft deflecting solely from the surface.

A model piled raft in soil was the subject of an experimental program by Garhy et al. in 2013. Rafts that were single-piled, unpiled, or placed on one of four, nine, or sixteen piles were all examined. The results showed that even a few piles beneath the center of the raft can improve its capacity for holding weight, and that the benefit increases with both the number of piles and their L/D slenderness ratio.At settlements of 10 mm and 25 mm, the load improvement ratio, or LIR, increases with the quantity of piles that reduce settlement as well as the L/D ratio. The relative stiffness of the raft (i.e., raft thickness) has a little effect on average settlement and the distribution of load between the raft and the piles.

Based on centrifuge load testing and a normalized non-linear load settlement relationship, Lee et al. (2014) proposed a settlement-based load-sharing model for piled rafts. They discovered that, at rates based on the load capacity ratio, the load-sharing ratio decreases as settlement increases.

Unsever and Matsumoto (2015) used an elastic model to simulate the raft and pile while employing a hardening soil model to model the sand. In consolidated drained triaxial testing on sand samples, pile parameters were established by simple bending tests, while soil parameters were evaluated. The findings indicated that the behavior of a placed raft is significantly influenced by both the applied load level and the interaction of its components, such as a raft and several piles beneath it. The behavior of piled raft foundations is significantly influenced by the raft component, including vertical load transmission by the raft that increases soil stress. The weight of pile elements varies according to the stress increment during vertical and horizontal loading.

Tschushingg and Schweiger (2015) proved that the improved embedded pile method is suitable for the different types of analysis, with the large number of deep foundations.

Elwakil and Azzam (2016) used experimental and numerical analysis to study the different characteristics of different parameters used in pile raft foundation. It has been found that the load carried by a raft increases as pile length and number decrease. The best and most ideal settlement ratio (S/B%) for designing the piled raft as a settlement reduction is also discovered to be 0.7%. At S/B = 0.7%, the final result shows that 39% of the load is carried by the raft.

Tradigo et al . (2016) analysed disconnected piles and raft and concluded that embedded pile(EP) and fully solid (FS) both results were similar and the reproduced load transfer through the gap soil.

In order to study the impact of earthquakes on the pile raft foundation, Kumar et al. (2016) used numerical analysis along with the finite element analysis program plaxis 3d. He described how a piled-raft foundation was used in a Vietnam-based structure for holding raw materials. To provide an in-depth analysis of the interactions between the soil and the structure, the foundation has been modelled using geotechnical software with finite elements. According to the results of the modeling and tests, the raft's share of the overall vertical weight is between 23 and 31%. The final design was complemented by several analysis results, including axial load in the piles, tilt in the raft, and vertical and differential settlement.

Sinha and Hanna (2017) Performed Numerical analysis for Piled Raft Foundation by considering variation in pile length, pile spacing, pile size, raft thickness, effect of cohesion and angle of shearing resistance and found important conclusions such as raft settlement increases with increase in pile spacing, a thinner raft leads to non uniform load shared by piles, a thicker raft will decrease differential settlement etc.

Chandiwala and Vansanwala (2018) used a 3d finite element model to analyse the effects of soil structure in layered condition. According to Chandiwala et al. (2018), settlement reduces, load sharing ratio rises, shear force falls, bending moment rises, and axial force on pile rises as raft thickness grows.

Deb and Pal (2019) developed a predicted model using finite analysis to assess load sharing behaviour and interaction effects and form load settlement responses , load sharing parameters and load sharing ratio for different configurations of pile raft foundation. Then the predicted proposed models were used to obtain the overall factor of safety both in terms of safety and serviceability.

Maximum pressure, settlement, and differential settlement all show a decline as raft thickness increases, but only up to a certain point, according to Azhar et al. (2020).Additionally, as pile diameter grows, so does the load that a raft can support.

Reduced maximum pressure, settlement, and differential settling are effects of larger pile diameter. Maximum pressure, differential settling, and pile spacing all rise as pile spacing increases.

# Chapter 3: Methodology

## 3.1 Basis of CPRF

Combined Pile Raft foundation is a type of foundation system that combines both pile foundation and raft foundation. The basis of this foundation system is to distribute the structural loads of a building or structure over a larger area by transferring them through piles and a concrete raft.

In this system, piles are first driven into the ground to a specified depth to transfer the load of the structure to a deeper, more stable layer of soil or rock. Then, a concrete raft is constructed on top of the piles to distribute the load evenly over a larger area.

The concrete raft is designed to be thick enough to support the loads from the structure and to distribute these loads to the piles, which in turn transfer the loads to the deeper, more stable soil or rock layer. This foundation system is suitable for structures on soft, weak, or compressible soil where the use of conventional spread footings may not be effective.

### 3.1.1 Pile

A pile is a type of foundation system that is used to transfer the load of a structure to a deeper, more stable layer of soil or rock. Piles are typically long, slender columns that are driven or drilled into the ground and connected to the structure above.

Types of pile have been classified on the basis of following criteria:

1. Material:timber, steel ,concrete
2. Cross Section:circular,square,hexagonal
3. Mode of load transfer:bearing,friction,tension

It could also be classified on the basis of displacement of soil during installation of pile:displacement pile,and non displacement pile

Displacement pile: If a large volume of soil is displaced by the pile during installation. For example: driven,cast in place,timber pile.

Non-displacement pile: If it doesn’t lead to any displacement of soil. For example: bored cast in situ,bored precast pile.

Pile may be subjected to vertical loads or lateral loads or combination of loads.

### 3.1.1.1 Single pile

When a compressive axial load (Q) acts on a pile, then pile will resist the amount of load on the basis of limit of its shaft friction and base resistance.

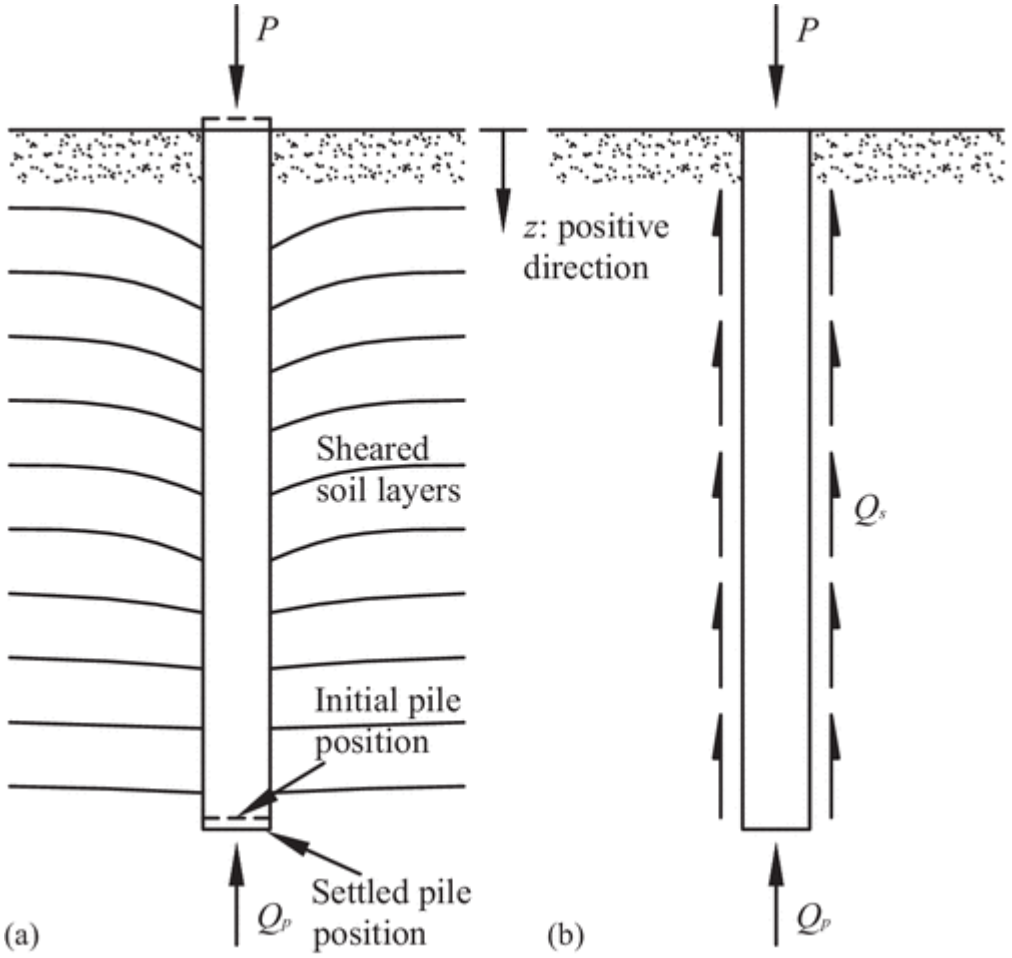


Figure 3.1 load transfer in single pile

The maximum load which a pile can resist is given by:

$Q_u = Q_{pu} + Q_f$ ----- (3.1)

Here,

$Q_{pu}$ = end bearing capacity

$Q_f$ = skin resistance

$Q_{pu}$ = $q_{pu}$ $A_b$ ----- (3.2)

Here,

$q_{pu}$ = end bearing resistance

$A_b$ = area of base of pile

For C – Ø soil:

$q_{pu} = cN_c + \sigma' N_q + 0.5\Upsilon BN_\Upsilon$ ----- (3.3)

here ,

c= cohesion

$N_c$ , $N_q$ ,$N_\Upsilon$ = bearing capacity factors

σ’ = effective overburden pressure at tip of pile

B = width or diameter of pile

$Q_f = f_s A_s$ ------(3.4)

Here,

$f_s$ = unit skin resistance

$A_s$ = suface area of pile

### 3.1.1.2 Pile Group

Number of piles forming a single block by a cap to resist the bending stress and increasing bearing capacity is called a pile group. The single pile couldn't accurately encounter or resist the eccentricity of load from structure as it might not cover the load in its zone of influence.In this case, we need to have pile group to strengthen the foundation.

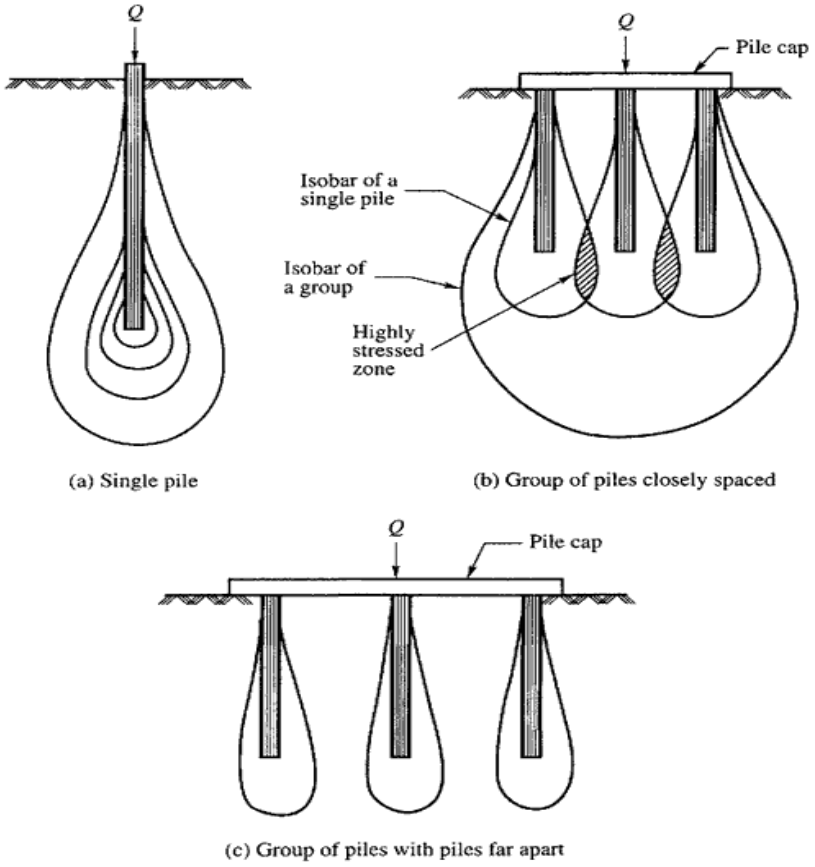


Figure 3.2 Stress distribution in group piles

The ultimate load capacity of the pile group by block failure is given by:

$$Q_{ug} = c_{ub} N_c A_b + P_b L cu' \text{ ------ } (3.5)$$

Here,

$Q_{ug}$ = ultimate load capacity of the pile group

cu' = average undrained strength of clay

$N_c$ = bearing capacity factor

$A_b$ = cross sectional area of block

$P_b$ = perimeter of block

L = embedded length of pile

$Q_{ug} = nQ_u$ ------ (3.6)

n = number of single piles

The ultimate load capacity of group is taken smaller of two values (3.5) and (3.6).

### 3.1.2 Raft

In situations where the ground beneath a building has a low ability to support weight and uneven settling is a concern, a raft can be used as a foundation. A raft is a solid slab that covers the entire footprint of the building, reinforced to support the loads from walls and columns.

**Bearing capacity of raft foundation:**

**a) Cohesionless soil**

As per Terzaghi's Theory, the modified ultimate bearing capacity for rectangular raft footing is:

$q_u = (1+0.3B/L)CN_c + \gamma D_f N_q + 1/2(1-0.2B/L)\gamma BN_\gamma$ --------(3.7)

Net Bearing capacity is given by,

$q_{nu} = q_u - \gamma D_f$ --------(3.8)

Where,

B = Width of footing

D = Depth of footing

L = Length of footing

C= Cohesion factor

$N_q$,$N_\gamma$ = Bearing capacity factor

$\gamma$ = Unit weight of soil

**b) Cohesive soil**

In cohesive soil, the net ultimate bearing capacity is generally determined using Skempton's equations and which is given as;

$q_{nu} = CN_C ( 1 + 0.2 D_f / B ) (1+0.2 B/L)$--------(3.9)

Where;

C = undrained cohesion

Nc = bearing capacity factor for footing at the surface

$D_f$= Depth of foundation

B = Width of raft

L = Length of raft

### 3.1.3 Combined Pile Raft Foundation

A combined pile raft foundation is a complex foundation system that consists of several components. The main components of a combined pile raft foundation include:

- Piles
- Raft
- Subsoil

The design and construction of a combined pile raft foundation require careful consideration of several factors, including the imposed load, the type and condition of the soil, and the groundwater level. The components of the foundation system must be designed and constructed to work together to provide a stable and secure foundation for the building or structure.

The load transfer mechanism in a combined pile raft foundation involves the transfer of the load of the building or structure through the raft to the piles, which transfer the load to a deeper, more stable layer of soil or rock.

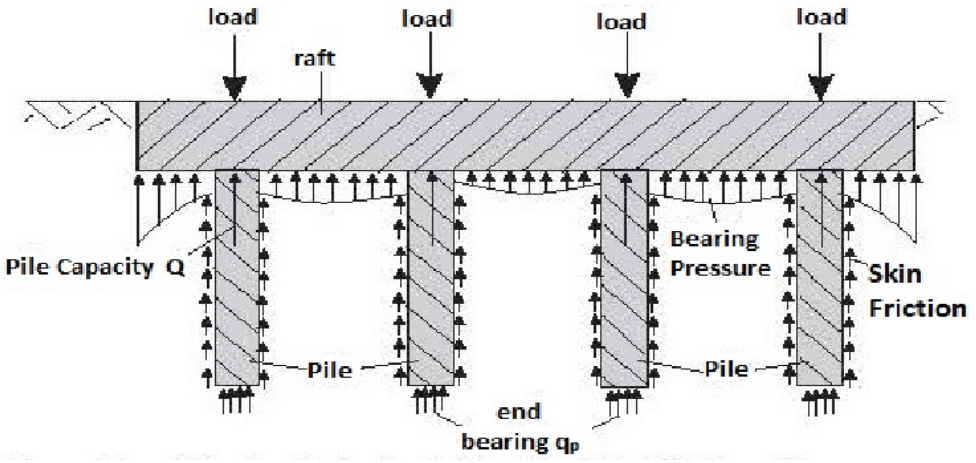


Figure 3.3 Load Transfer Mechanism of CPRF

### 3.1.3.1 Design Approach

Load bearing capacity of CPRF is the sum of capacities of raft and group piles. However, various interaction factors between the foundation and subsoil affect the capacities of raft and piles. (Kumar, 2016) suggested the equation for capacity of CPRF:

$$Q_{CPRF} = Q_{unpiled\ raft} + Q_{piles} \text{ ------- (3.10)}$$

Here,

$Q_{unpiled\ raft}$ = capacity of raft foundation

$Q_{piles}$ = capacity of group piles

Considering interaction factors the equation (1) modified to:

$$Q_{CPRF} = \alpha_{pr} Q_{\text{unpiled raft}} + \alpha_{rp}\, \alpha_{pp} \sum_{n=1}^{n} Q_{\text{single pile}} \text{ ---------( 3.11)}$$

Here,

$\alpha_{pr}$ = Pile to raft interaction

$\alpha_{rp}$ =Raft to pile interaction

$\alpha_{pp}$ = Pile to pile interaction

### 3.1.4 Efficiency of Pile Group

The efficiency of the load-bearing capacity of a group pile may be defined as

$$\eta = Q_{g(U)}/Q_{s(u)} \text{----------(3.12)}$$

Where,

$\eta$ = group efficiency

$Q_{g(U)}$ = ultimate load-bearing capacity of the group pile

$Q_{s(u)}$ = ultimate load-bearing capacity of each pile without the group effect

Efficiency of the pile group can be found by Feld's Rule, which reduces the capacity of each pile by 1/16 for each adjacent pile, by the empirical expression of Converse-Labarre or by the group reduction formula of (Terzaghi and Peck, 1967).

In Feld's Rule, act of the spacing of the piles is not taken into consideration. Widely used Converse-Labarre formula, for the efficiency E of the group, is expressed as;

$$E = 1 - \theta\{(n-1)m+(m-1)n\}/90mn \text{--------(3.13)}$$

Where,

m= number of columns of piles in a group.

n = number of rows,

$\theta = \tan^{-1}(d/s)$ in degrees.

d = diameter of pile.

s = spacing of piles centre to centre.

### 3.1.5 Bearing Capacity of Raft

The ultimate bearing capacity equations given by Terzaghi are for continuous, square, and circular foundations only; they do not address the case of rectangular foundations Also, the equations do not take into account the shearing resistance along the failure surface. In addition,the load on the foundation may be inclined. To account for all these shortcomings, (Meyerhof,1963) suggested the following form of the general bearing capacity equation:

$$q_u = c'N_cF_{cs}F_{cd}F_{ci} + qN_qF_{qs}F_{qd}F_{qi} + \tfrac{1}{2}*\gamma BN_\gamma F_{\gamma s}F_{\gamma d}F_{\gamma i} \text{ -------- } (3.14)$$

Where,

c' = cohesion

q= effective stress at the level of the bottom of the foundation

$\gamma$= unit weight of soil

B= width of foundation (= diameter for a circular foundation)

$F_{cs}$ ,$F_{qs}$,$F_{\gamma s}$= shape factors

$F_{cd}$, $F_{qd}$ ,$F_{\gamma d}$ = depth factors

$F_{ci}$, $F_{qi}$, $F_{\gamma i}$ = load inclination factors

$N_c$, $N_q$, $N_\gamma$ bearing capacity factors

### 3.1.6 Interaction Factors

To analyse the load capacity of CPRF, several researchers have given different approaches for calculation. Load capacity of CPRF can be calculated using load capacity of unpiled raft and pile group along with interactions factors that relate individual capacity with combined capacity.

It can be computed as the summation of the capacity of pile group (written in terms of individual pile capacities) and un-piled raft, multiplied with their interaction factors (Kumar and Choudhury, 2018)

$$Q_{CPRF} = \propto_{PR} \propto_{PP} \sum^{n}_{n=1} Q_{Single\ pile} + \propto_{RP} Q_{Unpiled\ Raft} \text{ ---------(3.15)}$$

Where,

$Q_{CPRF}$, $Q_{single\ pile}$ and $Q_{unpiled\ raft}$ are the load-bearing capacity of the CPRF, single pile and unpiled raft foundation.

$\alpha_{pr}$, $\alpha_{pp}$ and $\alpha_{rp}$ are pile-raft, pile-pile and raft-pile interaction factors.

**Estimation of Pile-Pile Interaction Factor ($\alpha_{pp}$)**

The pile-pile interaction is the result of pile group effect, defined as the changes in the load-settlement response of a pile group and single piles due to superimposition of stress and displacement field of a single pile in a group (Kumar and Choudhury,2018).

Load carrying capacity of single pile can be used to calculate load bearing capacity of pile group using this interaction factor as shown:

$$Q_{Group\ Pile} = \propto_{PP} \sum^{n}_{n=1} Q_{Single\ pile} \text{ --------- (3.16)}$$

**Estimation of Pile-Raft Interaction Factor ($\alpha_{pr}$)**

Load settlement of pile group changes when raft is placed above pile group. Load carrying capacity of pile group in CPRF $Q_{P\text{-}CPRF}$ is influenced by Pile-Raft interaction factor as shown below:

$Q_{P-CPRF} = \propto_{PR} Q_{Group\ Pile}$ -------- (3.17)

The estimation of this interaction considering both negative and positive aspects is very complex. The predicted values of αpr were limited to unity for conservatism in the design and expressed as (Kumar and Choudhury, 2018):

$$\propto_{PR} = (Q_{P-CPRF} / Q_{Group\ Pile}) = 1 - exp(-10.55\ (w/B_r)^{0.26}) \text{ -------- (3.18)}$$

Where,

w = Settlement of pile raft foundation

$B_r$ = Width of raft

**Estimation of Raft-Pile Interaction Factor ($\alpha_{rp}$)**

Load carrying capacity of the raft changes when a pile is introduced below the raft. The load carrying capacity of a raft of CPRF, $Q_{R-CPRF}$ can be computed in terms of load carrying capacity of an unpiled raft using this factor:

$Q_{R-CPRF} = \propto_{RP} Q_{Unpiled\ Raft}$ --------- (3.19)

$\propto_{RP}$ is expressed as the ratio of load carrying capacity of CPRF to the summation of the load-bearing capacity of the un-piled raft and the pile group (Kumar and Choudhury, 2018):

$\eta = Q_{CPRF} / (Q_{UP} + Q_{PG})$ --------- (3.20)

The value of η is calculated for all the configurations which indicate an increase in η with an increase in the normalised settlement ($w/B_r$). A generalised prediction equation was fitted with the obtained results using the method of least square as (Kumar and Choudhury, 2018):

$\eta = 3.5(w/B_r) - 0.06(S/D_p) - 0.5/D_p + 1.27$ --------(3.21)

Thereafter, an equation of $\alpha_{rp}$ is derived by using η and $\alpha_{pr}$ as (Kumar and Choudhury,2018):

$$\propto_{RP} = (Q_{R-CPRF} / Q_{Unpiled\ Raft}) = \eta + (\eta - \propto_{PR})(Q_{PG} / Q_{UR})$$ ------- (3.22)

### 3.1.7 Stiffness of Single Pile

The pile stiffness is easily calculated using two parts:

1. Soil Stiffness = Pile Capacity / Anticipated Settlement

2. Actual Pile Stiffness = PL / AE

with P being the pile capacity,

L being the length,

A being the pile area,

and E being the grout or steel modulus depending on the type of pile being used. (Felming et al., 1992) has stated the stiffness of the shaft and base of pile as;

Shaft stiffness of Pile:

$$\frac{P_s}{W_s} = \frac{2\pi}{\zeta} L\overline{G}$$ ---------(3.23)

Base stiffness of Pile:

$$\frac{P_b}{W_b} = \frac{2\, d_b g_b}{(1-v)}$$ -------(3.24)

For a stiff pile, the base settlement and shaft settlement will be similar to the settlement of the pile head, $w_t$.

The settlement of pile head $w_t$ under the load $P_t$ can be calculated by combining both of the above equations:

$$\frac{P_t}{w_t d G_l} = \frac{2 d_b G_b}{(1-v)} + \frac{2\pi}{\zeta} \frac{\overline{G}}{G_l} \frac{L}{d} \quad \text{---------(3.25)}$$

The stiffness of a pile may be written as;

$$K_p = \frac{P_t}{W_t} = \mathrm{d} G_l \left\{ \frac{2 d_b G_b}{(1-v)} + \frac{2\pi}{\zeta} \frac{\overline{G}}{G_l} \frac{L}{d} \right\} \text{----------(3.26)}$$

where,

$\zeta = \ln\{[0.25 + (2.5\rho(1-\nu) - 0.25)\zeta]\}\ 2L/d$ ---- (3.27)

When, $G_L = G_b$, $\xi = 1$

$\zeta = \ln[5\rho(1-\nu)L/d]$ ------ (3.28)

Where, $\rho = \overline{G}/G_L$ (variation of soil modulus with depth)

G is the shear modulus , $G_L$ and $G_b$ shear modulus of length and base

$\overline{G}$ is the average shear modulus of the soil over the embedded depth

L is length of the pile

d is diameter of pile

(Felming et al., 1992) further simplifies in appropriate boundary conditions at pile base yields an expression for load settlement ratio of the pile head:

$$\frac{P_t}{w_t d G_l} = \frac{\frac{2\eta}{(1-\upsilon)\xi} + \frac{2\pi\rho}{\zeta} \frac{tanh(\mu L)}{\mu L} \frac{L}{d}}{1 + \frac{8\eta}{\pi\lambda(1-\upsilon)\xi} \frac{tanh(\mu L)}{\mu L} \frac{L}{d}} \quad \text{---------(3.29)}$$

$\eta = d_b/d$ (ratio of underream for under reamed piles)

$\xi = G_L/G_b$ (ratio of end-bearing for end-bearing piles)

$\rho = \overline{G}/G_L$ (variation of soil modulus with depth)

$\lambda = E_p/G_L$ (pile-soil stiffness ratio)

$\zeta = \ln(2r_m/d)$ (measure of radius of influence of pile)

$\mu L = 2(2/\zeta\lambda)^{1/2}$ (L/d) (measure of pile compressibility)

### 3.1.8 Stiffness Of Group Pile

The stiffness, $K_g$, of the pile group (total load divided by average settlement) may be expressed as a fraction, $\eta_w$, of the sum of the individual pile stiffnesses, k. Thus for a group of n piles:

$$K=\frac{1}{R_s} = \frac{K_g}{\eta K_p} \quad \text{-----(3.30)}$$

Butterfield and Douglas plotted the efficiency, ηw, against the number of piles in a group gave essentially straight lines on logarithmic axes , showed that:

$$K_g = \eta_w nk$$

$$\eta_w \sim n^{-e} \quad \text{or} \quad K_g \sim n^{1-e}K$$

this results a group stiffness $K_g = n^{1-e}\,k$ -------- (3.31)

where, e is the efficiency exponent, it depends on the slenderness ratio of pile

### 3.1.9 Stiffness of Raft

Raft stiffness may be defined as a ratio of imposed stress to the resulting settlement.

Raft stiffness is given by (Davis, 1980)

$K_r = \frac{2.25GB}{(1-v)}$ ---------- (3.32)

Other authors have also suggested different relative stiffness factors for raft foundations. (Gupta, 1997) calculated the stiffness of raft with the underlying soil as ;

- Rectangular rafts: $K_r = \frac{E_r}{12E_s}\left(\frac{t}{B}\right)^3$
- Circular rafts: $K_r = \frac{E_r}{12E_s}\left(\frac{t}{B}\right)^3$

Where ,

$E_r$= Young's modulus of the raft

$E_s$= Young's modulus of the subsoil

B= length of the section in the bending axis

t= thickness of the raft

R= radius of the raft

### 3.1.10 Stiffness of Combined Piled – Raft Foundation

The stiffness of CPRF could be found by using a simple method of estimating load sharing capacity between raft and piles as outlined by Randolph (1994).

$K_{pr} = \frac{K_p + K_r(1-2\alpha_{rp})}{1-(\alpha_{rp}^{\ 2})(K_r/K_p)}$ ----------(3.33)

Where,

$K_{pr}$ =stiffness of piled raft

$K_p$ =stiffness of the pile group

$K_r$ =stiffness of the raft alone

$\alpha_{rp}$ = raft-pile interaction factor

### 3.1.11 Load Sharing Mechanism

The load shared by raft to the total load is calculated by using formula of (Fraser & Wardle, 1976),

$$X=\frac{P_r}{P_t}=\frac{P_r}{P_r+P_p}=\frac{(1-\alpha_{rp})K_r}{K_p+K_r(1-2\alpha_{rp}K_r)} \text{---------(3.34)}$$

Where,

$P_r$ = load carried by raft

$P_t$ = total load

$\alpha_{rp}$ = raft-pile interaction factor

From (Randolph, 1994)

$$\alpha_{rp}=1-\frac{ln(\frac{r_c}{r_o})}{\zeta} \text{---------(3.35)}$$

Where,

$r_c$ = Average radius of the pile cap

$r_o$ = Radius of the pile

$$\zeta = ln(\frac{r_m}{r_o})$$

$r_m = \{0.25 + \xi [2.5(1 - \nu) - 0.25\} * L$ ------(3.36)

$\xi = E_{sl} / E_{sb}$

$\rho = E_{sav} / E_{sl}$

L= Length of pile

$E_{sl}$ = Young's modulus of soil at level of pile tip

$E_{sb}$ = Young's Modulus of soil at bearing stratum below pile tip

$E_{sav}$ = Average Young's modulus of soil along pile shaft

### 3.1.12 Settlement of piled raft:

The settlement of piled raft can be evaluated using equation:

$Spr = \frac{Kr * Se}{Kpr}$

Where,

Spr = Settlement of piled raft

Kr = Raft Stiffness

Kpr = Piled raft stiffness

Se = Settlement of raft without pile under total load

## 3.2 Methodology for determining soil parameters

### 3.2.1 Water Content

The water content (w), is the ratio of the weight of water to the weight of the solids in a given mass of soil. This ratio is usually expressed as percentage. When voids are completely filled with air, water content is equal to zero (dry soil).
Water content was determined by the oven drying method. In this method, a known weight of soil was weighed and placed in an oven at a temperature of around 105°C to 110°C for a period of 24 hours. After 24 hours, the soil was removed from the oven and weighed again. The difference in weight was the weight of water that was originally present in the soil, which can be used to calculate the water content of the soil.

**Water content (%) = [(Wet weight - Dry weight) / Dry weight] x 100%**
where;
Wet weight: the weight of the soil sample before drying
Dry weight: the weight of the soil sample after drying in an oven at a specific temperature (usually 105-110°C) until it reaches a constant weight

### 3.2.2 Specific Gravity

The density bottle method was performed to determine the specific gravity of soil. The following steps were followed:
1. A specific gravity bottle of 100ml was cleaned and dried. Its weight was recorded.
2. The empty specific gravity bottle was weighed and its weight was recorded.
3. A representative soil sample of about 50 grams was taken and dried in an oven at a temperature of 110°C to 120°C until the weight of the soil sample remained constant.
4. A portion of the dry soil sample (about 10 grams) was weighed and its weight was recorded.
5. Distilled water was added to the specific gravity bottle until it was filled to the mark. The filled bottle was weighed and its weight was recorded.
6. The bottle was emptied and the dry soil sample was added to it. The bottle was filled with distilled water again until it was filled to the mark. The filled bottle was weighed and its weight was recorded.

7. The weight of water displaced by the soil was calculated by subtracting the weight of the filled specific gravity bottle from the weight of the filled specific gravity bottle containing soil and water.
8. The specific gravity of the soil was calculated using the formula:
**Specific gravity = (Weight of dry soil sample / (Weight of water displaced by the soil – Weight of empty specific gravity bottle))**.
9. The process was repeated with other soil samples and an average of the results was taken to obtain a more accurate value.

### 3.2.3 Bulk Density and Dry Density

Bulk density and dry density of soil was determined by the core cutter method. For this following procedure were done:

1. A representative soil sample from the location of interest was collected.
2. Mass of the empty core cutter was recorded.
3. The core cutter was driven into the soil vertically until it reached a suitable depth (usually about 5 to 10 cm) using a hammer.
4. Straightedge was used to level the soil surface with the rim of the core cutter, ensuring that there are no air gaps or voids.
5. Ruler was used to measure the height and diameter of the soil sample within the core cutter and record the values.
6. The soil sample from the core cutter was removed and weighed. The mass of the wet soil sample was recorded.
7. Sample was oven dried to remove moisture.
8. The soil sample was weighted again and recorded the mass of the dry soil sample.
9. The bulk density of the soil was calculated using the formula: **Bulk density = Mass of wet soil sample / Volume of soil sample (i.e., the volume of the core cutter)**
10. The dry density of the soil was calculated using the formula: **Dry density = Mass of dry soil sample / Volume of soil sample.**

### 3.2.4 Liquid Limit

The liquid limit of soil was determined using the following steps:

1. About 120 grams of air-dried soil was taken and placed in a mixing bowl.

2. Distilled water was added to the soil in increments and mixed thoroughly until a smooth paste was obtained.

3. The paste was transferred to the cup of the liquid limit apparatus.

4. A groove-making tool was used to make a groove in the soil paste, and then the cup was closed by rotating the crank at a rate of about 2 revolutions per second.

5. The number of blows required for the two halves of the groove to close at a distance of 13 mm using a standard liquid limit device was recorded.

6. The test was repeated with additional soil samples to obtain three or more values.

7. Then a flow curve between logN and w was drawn and water content corresponding to 25 blows was recorded

8. The resulting water content is the liquid limit of soil.

It was important to ensure that the soil was thoroughly mixed with the water and that the groove-making tool was of the appropriate size to ensure accuracy.

### 3.2.5 Plastic Limit

The plastic limit of soil is defined as the minimum moisture content at which soil can be rolled into a thread 3mm in diameter without breaking.

To determine the plastic limit of soil, a soil sample was taken and mixed with distilled water to form a uniform paste. The paste was placed on a clean porcelain plate and divided into two halves. One half was rolled with fingers on the plate until it formed a 3 mm diameter thread. This process was repeated with the other half of the paste, adding small amounts of water until the thread could be formed without breaking. The moisture content of the soil paste was recorded when the thread just started to break. The process was repeated with other soil samples to obtain an

average value. The test should be conducted immediately after soil collection to obtain accurate results.

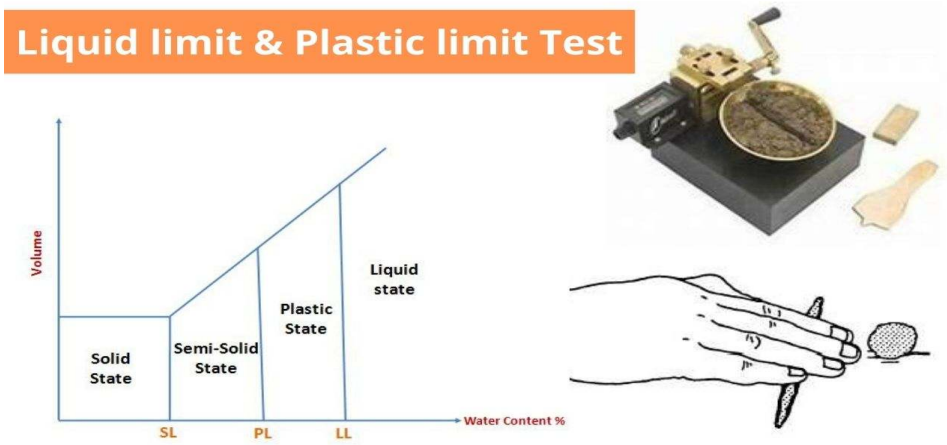


Figure 3.4 Liquid Limit and Plastic limit test

### 3.2.6 Sieve Analysis

Sieve size analysis of soil was performed for coarse and fine soil as per following procedures:

Part-I: Coarse Sieve Analysis

1. Required quantity of sample was taken and sieved through 4.75mm IS sieve. Soil retained on it was taken for coarse sieve analysis and soil particles passing through it was taken for fine sieve analysis.
2. The material retained on the sieve was rubbed with pestle on mortar with care such that individual particles shall not break. Amount of material taken for sieving on each sieve should be such that the maximum mass of soil retained on each sieve does not exceed the specific value.
3. Mass of the material retained on each sieve was determined.
4. The percentage of soil retained on each sieve on the basis of total mass of sample in step 1 was calculated.
5. The percentage passing through each sieve was determined.

Part -II: Fine Sieve Analysis

1. Soil sample passing through 4.75mm IS sieve was taken. It was oven dried at 100° to 105°C and weighted it to 0.1% of total mass.
2. The soil was sieved through the nest of fine sieves and agitated in irregular motion.
3. The material retained on the sieve was rubbed with pestle on mortar with care such that individual particles shall not break.

4. The material was received through the nest of sieves. Minimum of 10 minutes of shaking was done.
5. The soil fraction retained on each sieve was collected in a separate container and mass was noted.
6. The percentage retained, cumulative percentage retained and percentage finer based on total mass taken in step 1 was calculated.
7. The particle size distribution curve was plotted by plotting the percentage passing on the y-axis and the sieve size on the x-axis.

Here before conducting step 2 of fine sieve analysis, water was added to the soil fraction, the mix was stirred thoroughly and left for soaking. The soaked specimen was washed on a 75 micron sieve until the water passing the sieve was clear. The fraction retained on the sieve was taken and dried in an oven. The oven dried was sieved through nest of fine sieves as discussed in step 2. Other steps were performed as before.

Obviously, the mass of material which would have been retained on the sieve was taken as original mass of soil before washing minus the dry mass of soil retained on 75 micron sieve after washing.

The particle size distribution curve could be used to classify the soil according to standard classification systems and to determine its engineering properties such as permeability, compressibility, and shear strength.

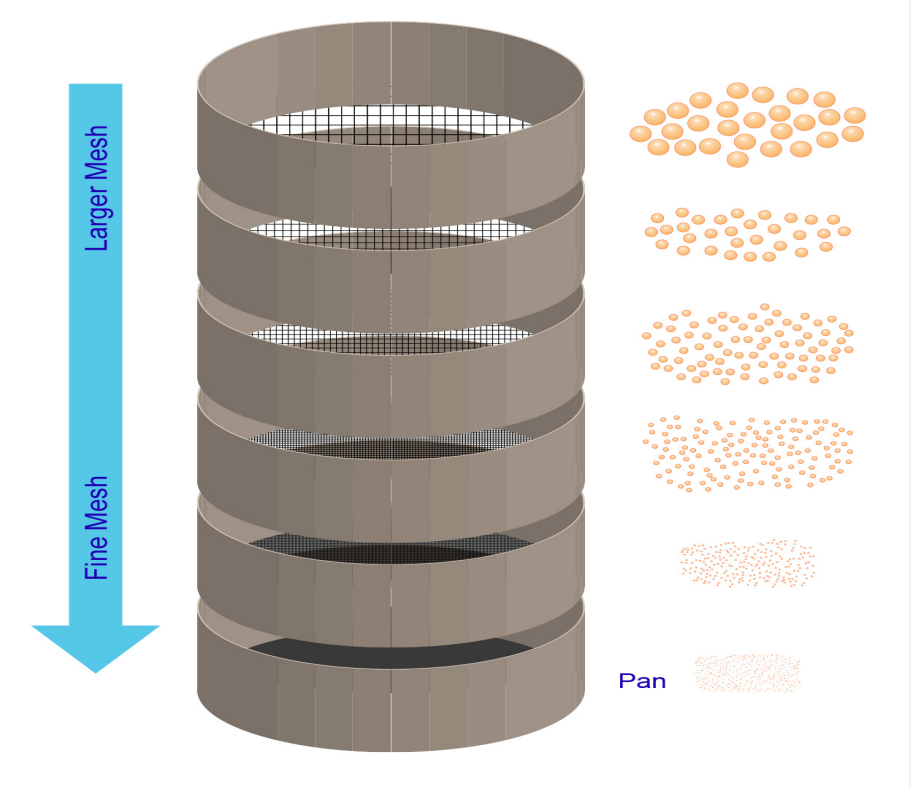


Figure 3.5 Sieve Analysis

### 3.2.7 Hydrometer Test of Soil

The hydrometer test is used to determine the particle size distribution of soil. We could split gravel and sand from the sieve analysis test however to determine the amount of silt and clay in the soil sample, a hydrometer test is required.

A representative soil sample was collected and dried in an oven to a constant weight. The dry soil sample was then crushed and sieved through a set of standard sieves to separate it into different particle size fractions.The hydrometer was calibrated to give readings of specific gravity. A known weight of the soil sample was added to a known volume of water in a graduated cylinder. The mixture was then stirred vigorously to create a suspension. The hydrometer was then inserted into the suspension and the specific gravity reading was taken after a specified time interval (30 sec,1, 2, 4, 8, 15, 30 minutes,1hr,2hrs,4hrs,8hr and 24hrs ). The specific gravity readings were then plotted on a graph, and the particle size distribution was determined using standard procedures. The hydrometer test is a relatively quick and easy method to determine the particle size distribution of soil, but it requires careful attention to detail to obtain accurate results.

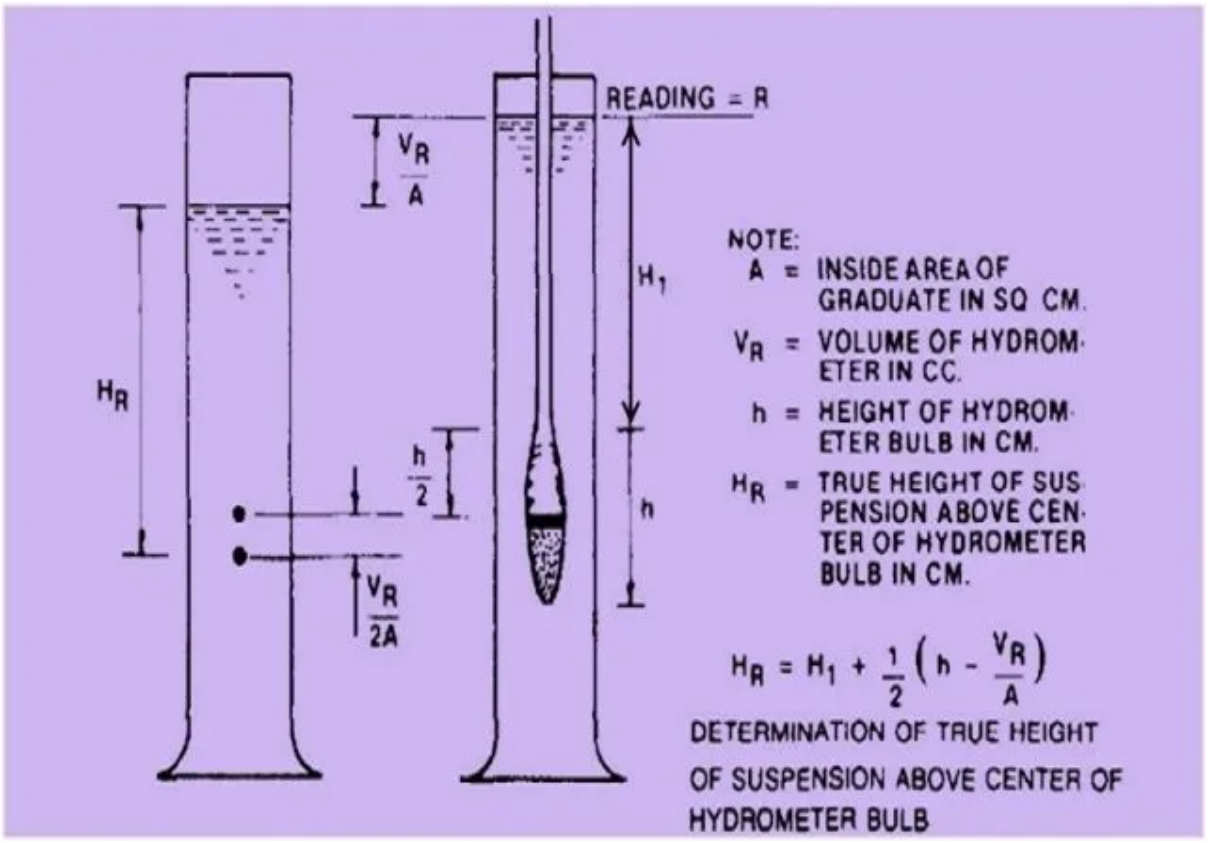


Figure 3.6 Hydrometer test of soil

### 3.2.8 Direct Shear Test

The direct shear test is used to determine the shear strength parameters of the soil.

The direct shear test was conducted using the following steps:

1. The soil sample was trimmed to the desired size and shape to fit the direct shear apparatus.

2. The direct shear apparatus was assembled and a normal load was applied to the soil sample through the loading piston.

3. The shear force was then applied to the soil sample by moving the horizontal shear box at a constant rate until the sample failed.

4. During the test, the vertical displacement and the horizontal displacement of the soil sample were measured.

5. The shear strength parameters, including the shear strength, angle of internal friction, and cohesion, were calculated based on the applied load, the dimensions of the soil sample, and the measurements of the vertical and horizontal displacements.

6. The test was typically repeated for several different normal stress levels to determine the shear strength parameters over a range of stress conditions.

The direct shear test is a simple and commonly used method for measuring the shear strength of soils in a laboratory setting. The results obtained from the test can be used to design foundations, slopes, and other geotechnical structures that rely on soil shear strength.

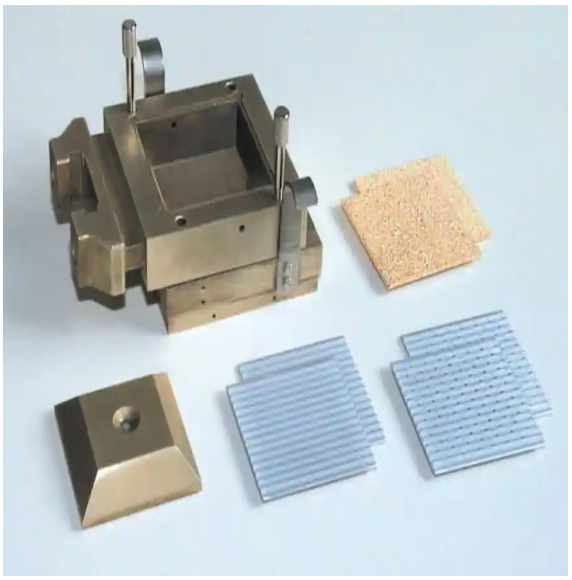

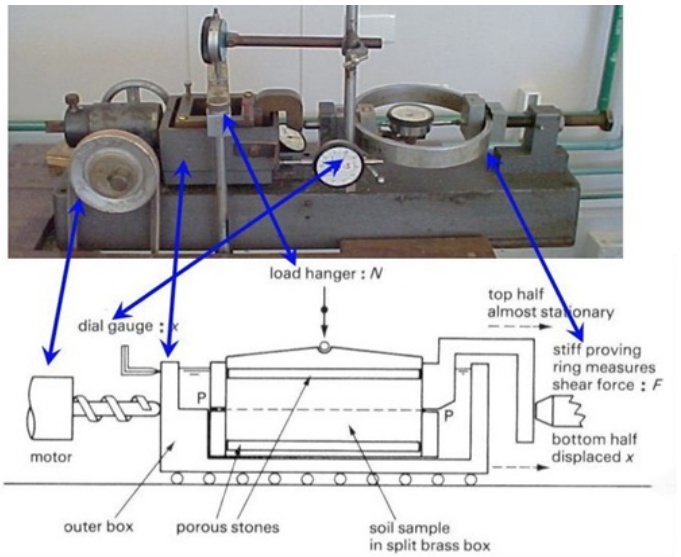


Figure 3.7 Direct Shear Test

### 3.2.9 Unconfined Compression Test

The undrained unconfined compression test was conducted using the following steps:

1. The soil sample was prepared and placed in a cylindrical mould with a fixed diameter and height.

2. The mould was placed in the compression testing machine and a vertical load was applied at a constant rate until the sample failed.

3. During the test, the axial strain and axial stress of the soil sample were measured.

4. The shear strength parameters, including the unconfined compressive strength and cohesion, were calculated based on the applied load and the dimensions of the soil sample.

5. The test was typically repeated for several different soil samples to obtain an average value of the shear strength parameters.

The undrained unconfined compression test is a simple and commonly used method for measuring the shear strength of soils in a laboratory setting. The results obtained from the test can be used to design foundations, slopes, and other geotechnical structures that rely on soil shear strength.

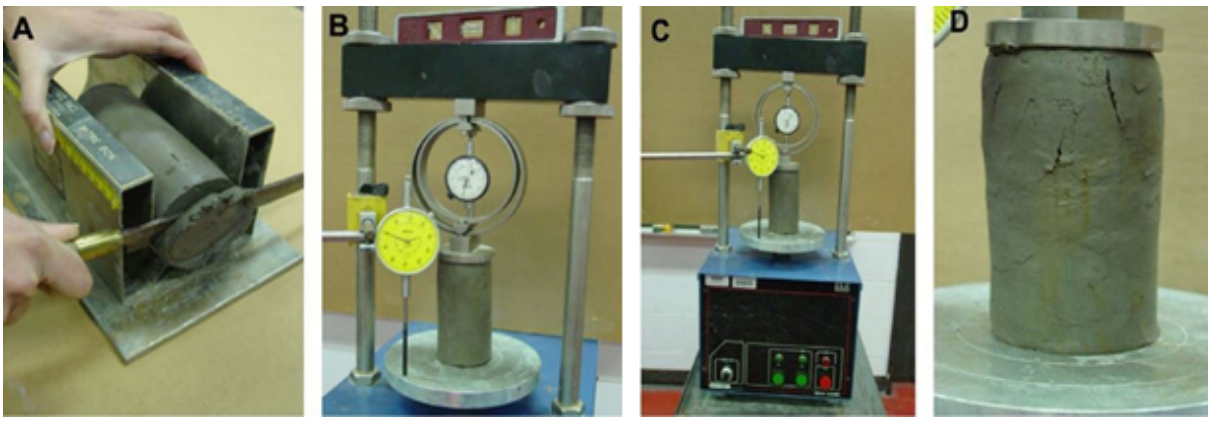


Figure 3.8 Unconfined Compression Strength Test

### 3.3 Flow Chart

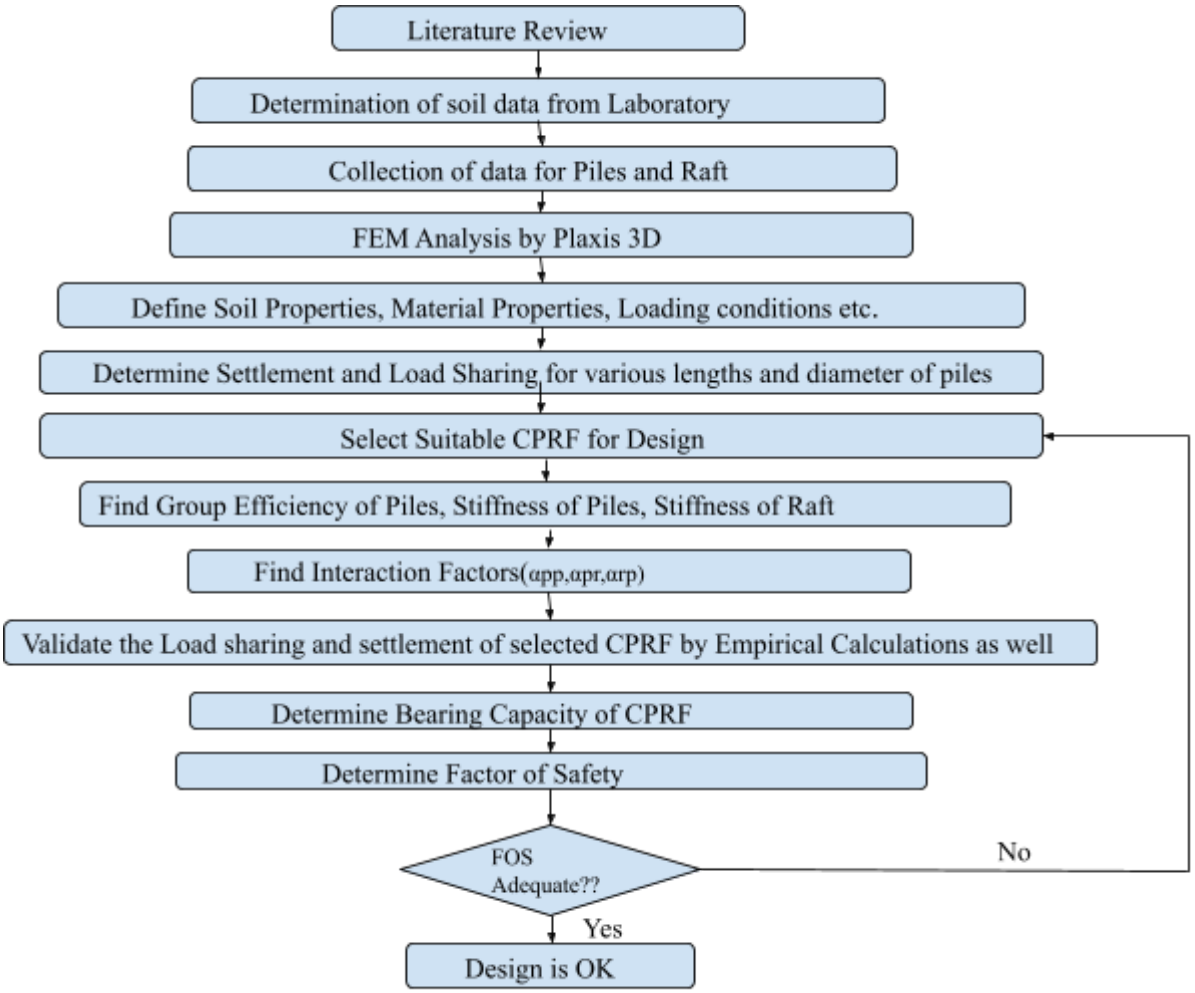

### 3.4 Finite Element Program: PLAXIS 3D

Plaxis 3D is a computer program that helps geotechnical engineers design and analyse structures like foundations, tunnels, and retaining walls. It does this by breaking down the structure into small parts and simulating how they will behave when they are put under pressure or stress. The software has tools for creating 3D models of the structures, simulating different types of soil and rock materials, and analysing the results. Plaxis 3D is used in many different types of engineering projects where soil and rock mechanics are important.

It consists of several main components:

1. Main Menu: This is located at the top of the interface and contains various menus for accessing the different features and tools of the software.
2. Project Workspace: This is the main area where users can create and manage their projects. It contains several tabs for creating and editing the model, defining the analysis settings, and viewing the simulation results.
3. Object Inspector: This is located on the right side of the interface and provides access to the properties and settings of the objects in the model. Users can select objects in the model workspace and view and edit their properties in the object inspector.
4. Toolbars: These are located at the top and sides of the interface and provide quick access to commonly used features and tools.
5. Graphical Display: This is the main area of the interface where users can view the 3D model and simulation results. Users can interact with the model and results using a variety of tools, such as pan, zoom, and rotate.

The user interface consists of two sub-programs: Input and Output.

1. Input: The input of Plaxis 3D refers to the data and information provided by the user to create a 3D model of the geotechnical structure being analysed. This input includes several components:
    a. Geometry Modelling: Plaxis 3D allows users to create 3D models of the structure using various geometry modelling tools. This includes creating shapes, volumes, and surfaces, importing external models, and defining coordinate systems.
    b. Material Properties: The software offers several material models for simulating the behaviour of different types of soil and rock materials. Users can define the material properties, including strength, stiffness, and density, and assign them to the appropriate parts of the model.
    c. Boundary Conditions: Plaxis 3D allows users to apply different boundary conditions to the structure, such as loads, displacements, and fixed constraints. Users can also define different stages of loading and analyse the behaviour of the structure at each stage.

d. Excavation: If the model involves excavation, Plaxis 3D offers tools for modelling the excavation process and its impact on the surrounding structures.
e. Analysis Settings: Users can define various analysis settings, including numerical methods, convergence criteria, and analysis types.

2. Output: The output of Plaxis 3D depends on the specific analysis that was performed, but generally includes:
    a. Deformation: Plaxis 3D provides information on the amount and direction of deformation in the soil and structures due to applied loads.
    b. Stress: The software calculates the stress distribution in the soil and structures under loading conditions, which can be used to assess the safety of the structure.
    c. Settlement: Settlement analysis is performed to determine the degree of settlement that can occur in the soil due to applied loads.
    d. Pore water pressure: Plaxis 3D computes pore water pressure and its distribution in the soil due to various loads and boundary conditions.
    e. Shear strength: The software computes the shear strength of soil at different depths, which is a critical parameter in geotechnical design.
    f. Safety factor: Plaxis 3D calculates safety factors for various failure modes such as slope stability, bearing capacity, and retaining walls.
    g. Visualisation: The software provides 3D visualisation of the analysed model, which allows engineers to understand the behaviour of the soil and structures under various loads.
    h. Time-dependent behaviour: Plaxis 3D also has the capability to model time-dependent soil behaviour, such as creep and consolidation.

### 3.4.1 Research Method and Sequence of Work Carried out in PLAXIS 3D Analysis

#### 3.4.1.1 Project Properties

The project properties of the analysis are tabulated in table 3-1.

| | | |
|---|---|---|
| Type | Model | Full |
| Type | Elements | 10-Noded |
| Units | Length | m |

| | | |
|---|---|---|
| Units | Force | kN |
| Units | Time | Day |
| Units | Stress | $kN/m^2$ |
| Units | Weight | $kN/m^2$ |
| General | Gravity | 1.0 g |
| General | Earth Gravity | 9.81 $m/s^2$ |
| General | $\gamma_{water}$ | 10 $kN/m^3$ |
| Contour | Xmin | -50.00 m |
| Contour | Xmax | 50.00 m |
| Contour | Ymin | -50.00 m |
| Contour | Ymax | 50 m |

Table 3.1 Project Properties of analysis

The project properties are to be inserted in PLAXIS 3D which is shown in figure below:

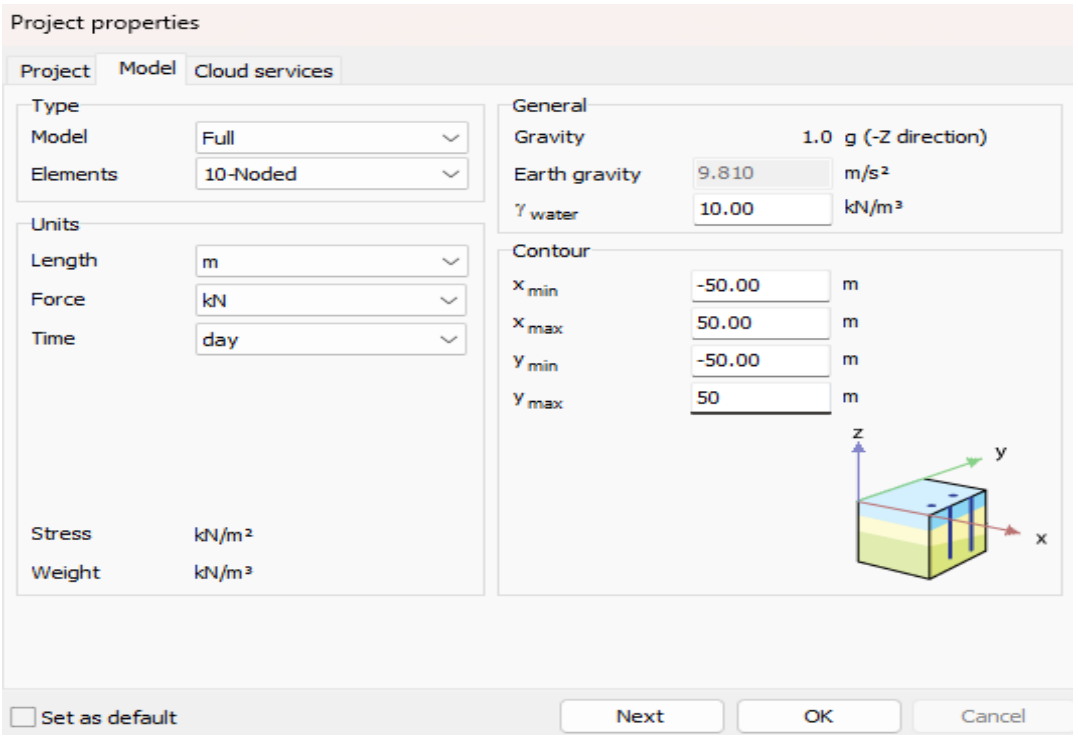


Figure 3.9 Project Properties Window in PLAXIS 3D

### 3.4.2 Properties of Soil

The properties of soil determined in lab which are required for simulation in Plaxis 3D are tabulated below. These values were assigned with the help of borehole option available in the software. The general groundwater table was assumed to be located at 3 meters from the ground surface. Also the soil was modelled with the help of Mohr-Column failure criteria.

| Parameters | Symbol | Soil |
|---|---|---|
| Material model | - | Mohr-Column |
| Unsaturated weight | ɣunsat | 17.45 |
| Saturated weight | ɣsat | 17.78 |
| Stiffness | E’ | 3315 |
| Cohesion | c’ref | 13.86 |
| Friction angle | Φ’ | 25.58 |
| Poisson's Ratio | ν' | 0.267 |
| Drainage Type | - | Drain |

Table 3.2 Properties of soil

### 3.4.3 Structural Properties

- Area of the building: 36 m * 36 m
- Location of Raft below ground surface: 2.5 m
- Thickness of Raft: 0.6 m
- Water Table below ground surface: 3m

### 3.4.3.1 Materials and Properties of Pile

The piles used in this experiment were assumed to be concrete piles with 1.5% steel reinforcement. In this experiment a number of piles were used and the variation of settlement and load sharing due to different length and spacing of piles was analysed. The properties of piles used are as follows:

| Parameters | Symbols | Value | Unit |
|---|---|---|---|
| Material Mode | - | Linearly Elastic | - |
| Unit Weight | ɣ | 25 | $kN/m^3$ |
| Stiffness | Eref | 2.78E+07 | $kN/m^2$ |
| Diameter | D | 1 | m |
| Length | L | 6D,9D,12D,15D | m |
| Spacing | S | 2D,3D,4D,6D,10D | m |

Table 3.3 Material and properties of pile

### 3.4.3.2 Material and Section properties of Raft

In this experiment the raft was assumed to be a concrete raft with 1.5% steel reinforcement. The properties of raft used in this analysis are as follows:

| Parameters | Symbols | Value | Unit |
|---|---|---|---|
| Material Mode | - | Linearly Elastic | - |
| Unit Weight | ɣ | 25 | $kN/m^3$ |
| Elastic Modulus | E | 2.78E+07 | $kN/m^2$ |
| Thickness | D | 0.6 | m |
| Length | L | 36 | m |
| Breadth | B | 36 | m |

Table 3.4 Material and section properties of Raft

### 3.4.4 Definition of Model and its Geometrics

The boundary conditions that were applied include the following:

1. The ground surface is unrestricted in all directions.
2. The bottom boundary of the model is fixed in all directions.
3. The vertical boundaries of the model that have their normal in the x direction are fixed in the x direction, but free in the y and z directions.
4. The vertical boundaries of the model that have their normal in the y direction are fixed in the y direction, but free in the x and z directions.
5. The vertical boundaries of the model that have their normal in the z direction are fixed in the z direction, but free in the y and x directions.

### 3.4.5 Loading conditions on CPRF

The footing is symmetrical to both x-axis and y-axis. Uniform loading is applied into the foundation.

Equivalent surface load = 100 $kN/m^2$

Total load of the structure at the centre = 100*(36*36)= 129600 kN

### 3.4.6 Method of Modelling of Pile

Piles can be modeled in two ways:

1. Analysis by Volume Element Method
2. Analysis by Embedded Beam Method

The main difference between Volume Element and Embedded Beams is the mesh created by model. When using Volume Element, the diameter and cross-sectional area and interfaces can be defined accurately whereas the embedded beam uses the equivalent diameter. Although, volume element can give accurate simulation some meshing problems might be encountered and calculation takes more time and consumes more PC resources. So, in this project most of the analysis is done by embedded beam method.

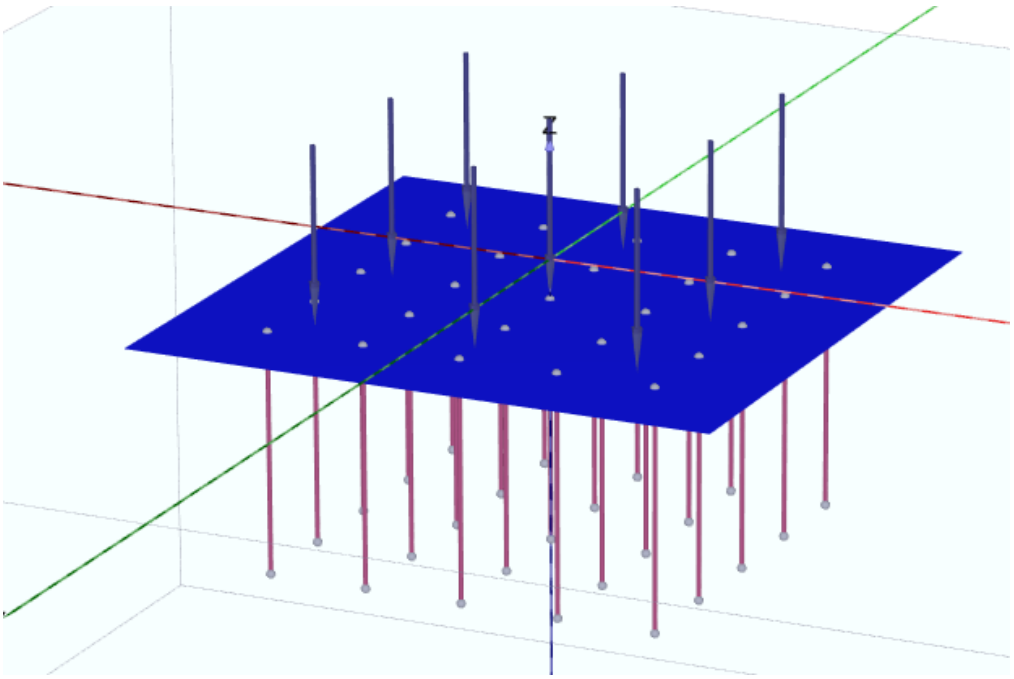


Figure 3.10 Analysis by Embedded Beam Method

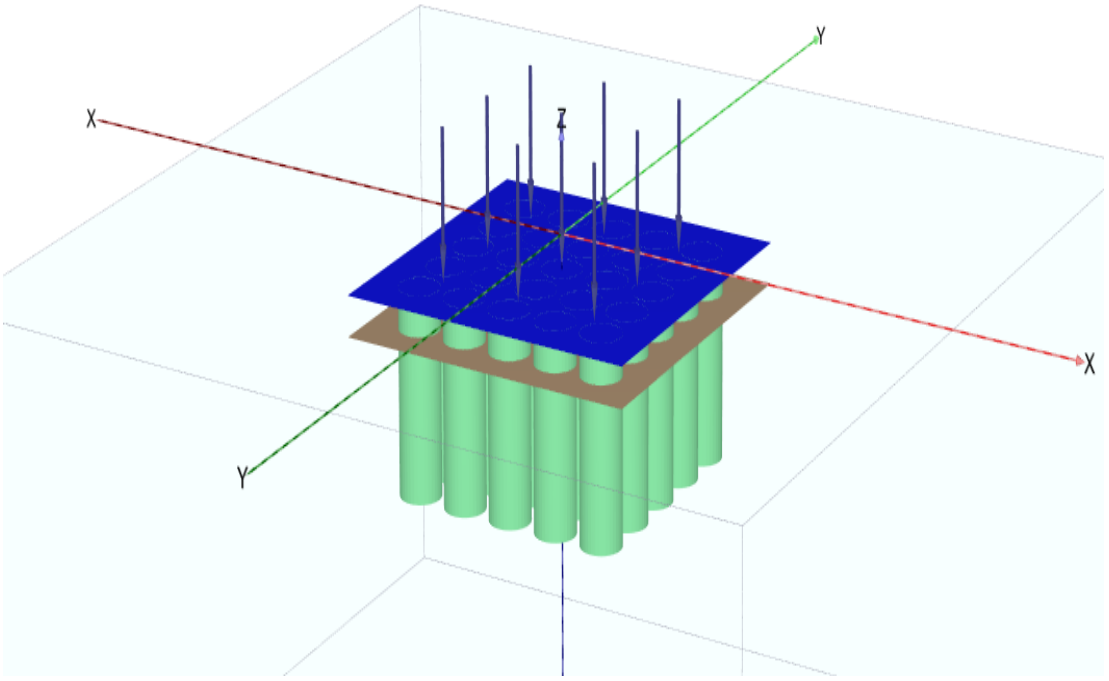


Figure 3.11 Analysis by Volume Element Method

### 3.4.6 General layout of model:

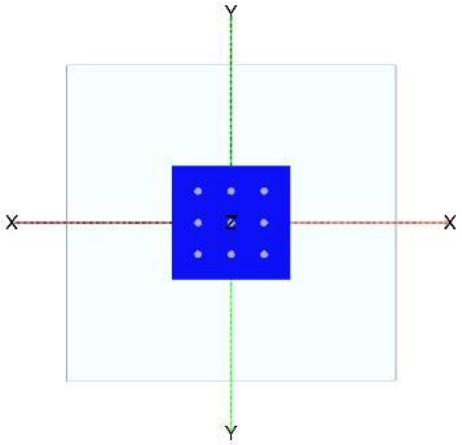


Figure 3.12 Layout with pile Spacing 10D

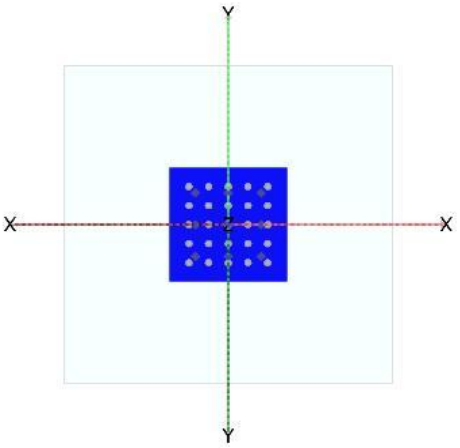


Figure 3.13 Layout with pile Spacing 6D

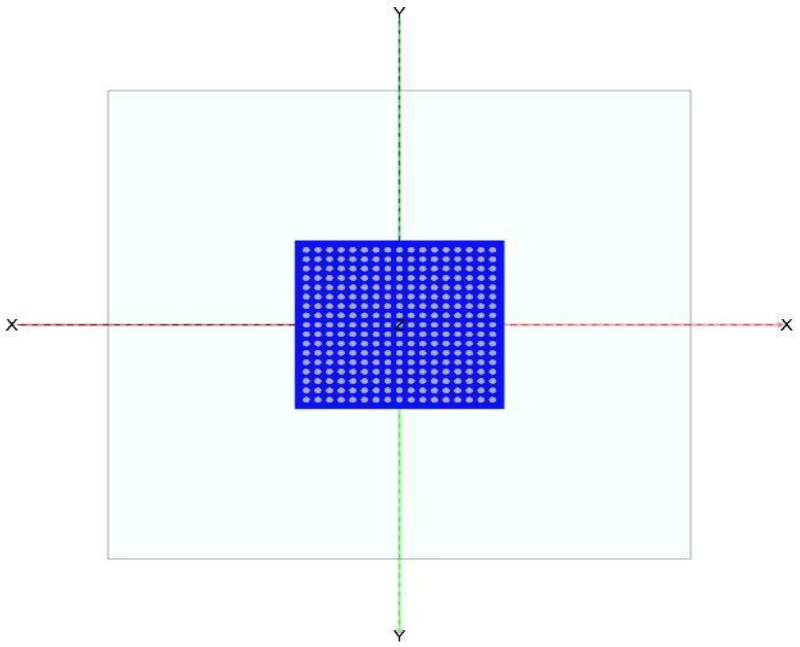


Figure 3.14 Layout with Pile spacing 2D

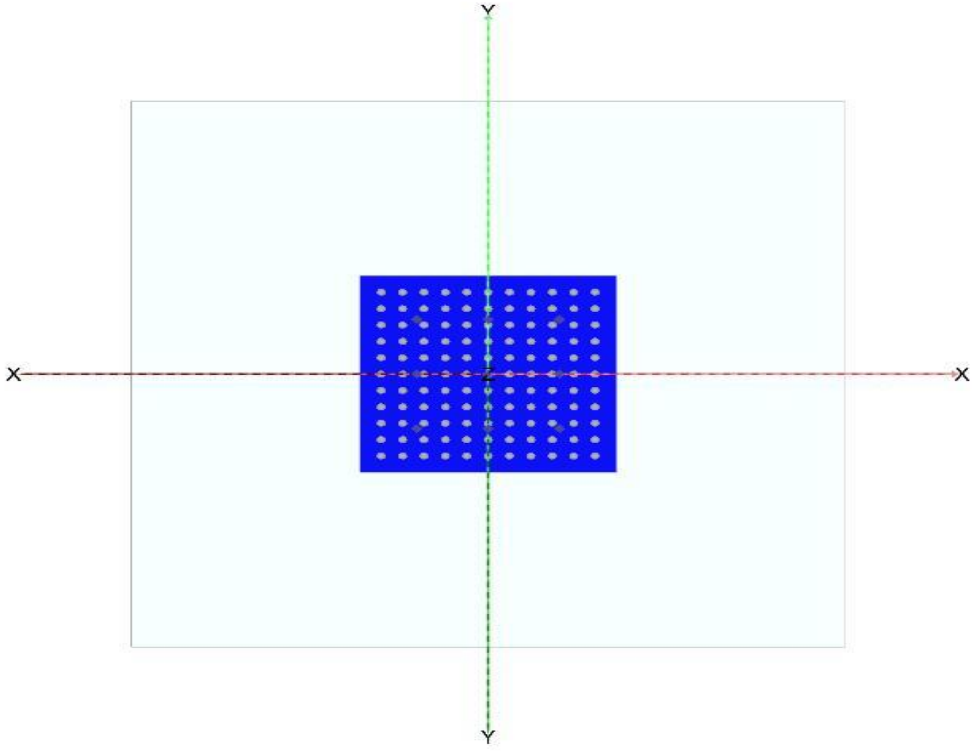


Figure 3.15 Layout with Pile spacing 3D

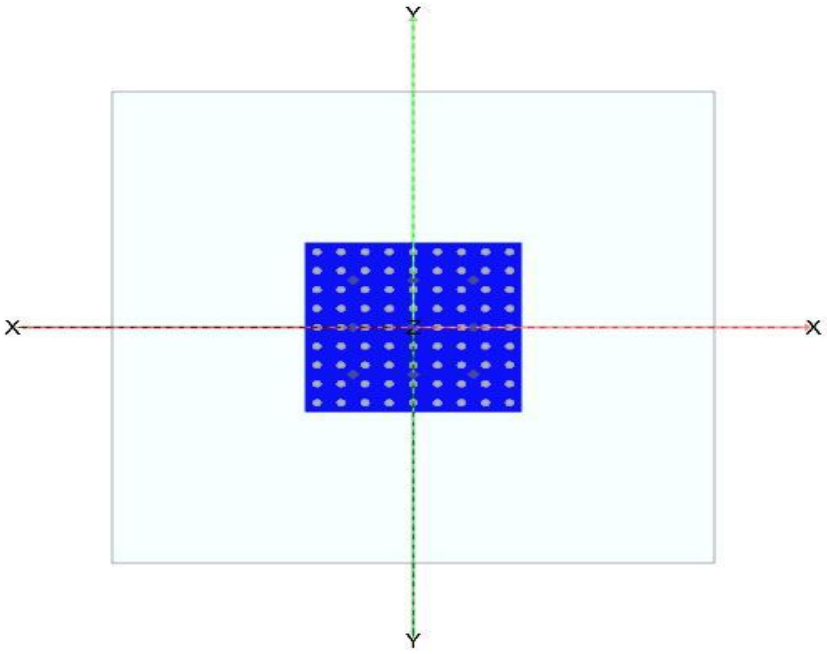


Figure 3.16 Layout with Pile spacing 4D

### 3.4.7 Validation of FEM modelling:

The validation of FEM modelling is confirmed using the finite element model developed by Sinha and Hanna 2016. The FE model developed in this study by Plaxis 3D is compared with the model developed by Sinha and Hanna and results are compared. For this purpose, a square sized raft model of 24*24m is chosen. The thickness of Raft is taken as 2m. The lengths of piles is taken as 5m and 15m,the diameter of piles was taken 1m, 16 piles were used for each case and the piles were spaced at 6 times the diameter. The properties of soil taken for validation purposes are also tabulated below. The graph below shows the comparison of results from Sinha and Hanna and our current model. It is clearly evident from the figure that the developed model shows very good agreement with the results from the reference model. Hence the given graph confirms the validity of numerical models used in our study.

| Parameter | Unit | Soil | Pile | Raft |
|---|---|---|---|---|
| Young's modulus, E | MPa | 54 | 25000 | 34000 |
| Poisson's ratio v | | 0.15 | 0.2 | 0.2 |
| Unit weight γ | $kN/m^3$ | 19 | 25 | 25 |
| Submersive unit weight γ' | $kN/m^3$ | 9 | 15 | 15 |
| Angle of internal friction Φ | ° | 20 | | |
| Cohesion c' | kPa | 20 | | |

Table 3.5 Material Properties used in the validation(Sinha and Hanna 2016)

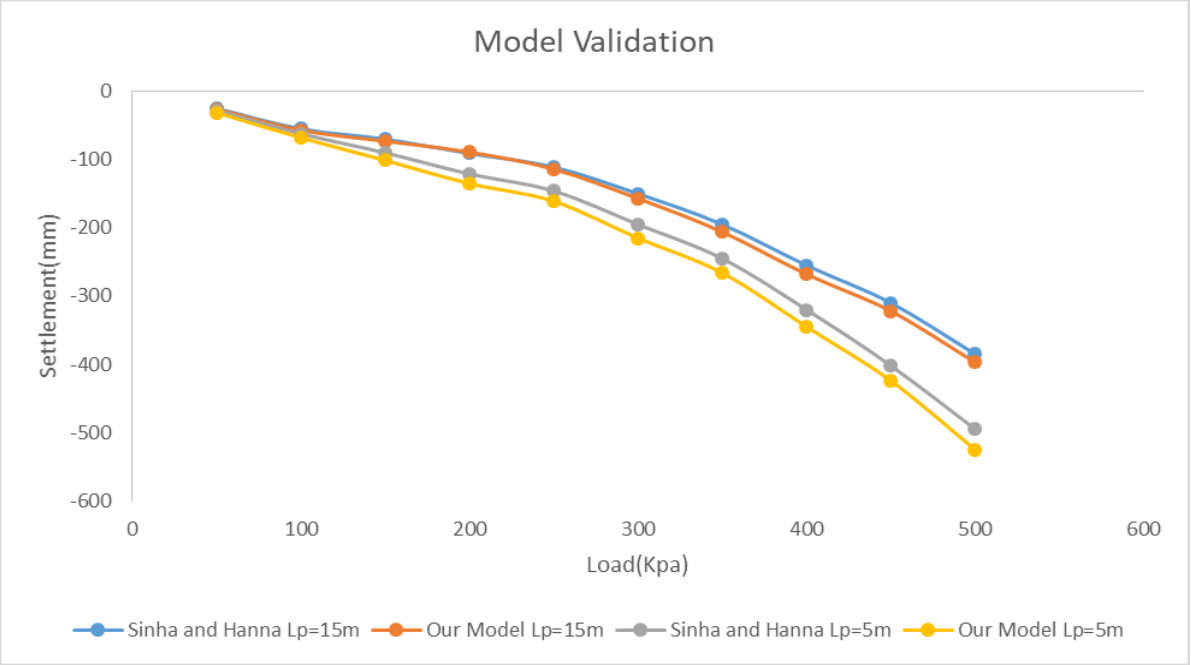


Figure 3.17 Comparison of load settlement behaviour of current model with Sinha and Hanna(2016)

# Chapter 4: Results and Findings

## 4.1 Variation of Settlement

The values of settlement at different Length and Spacing of piles is given below:

| Depth | 2D Spacing Settlement | 3D Spacing Settlement | 4D Spacing Settlement | 6D Spacing Settlement | 10D Spacing Settlement |
|---|---|---|---|---|---|
| 6D | 54.55 | 72.38 | 92.58 | 124.07 | 175.73 |
| 9D | 52.68 | 60.54 | 71.47 | 94.54 | 142.22 |
| 12D | 51.28 | 55.17 | 64.14 | 84.05 | 125.37 |
| 15D | 48.72 | 51.12 | 58.27 | 75.32 | 112.46 |

Table 4.1 variation of settlement at different length and spacing of piles

Here, D is the diameter of piles which is 1m and all the settlement values are in mm.

### 4.1.1 Variation in settlement of CPRF with Spacing of Piles

For this, The piles were spaced at 2D,3D,4D,6D and 10D spacings and the values of settlements were determined using Plaxis 3D software and a graph was plotted, plotting spacing in X-axis and Settlement in Y-axis. The resulting graph is shown below.

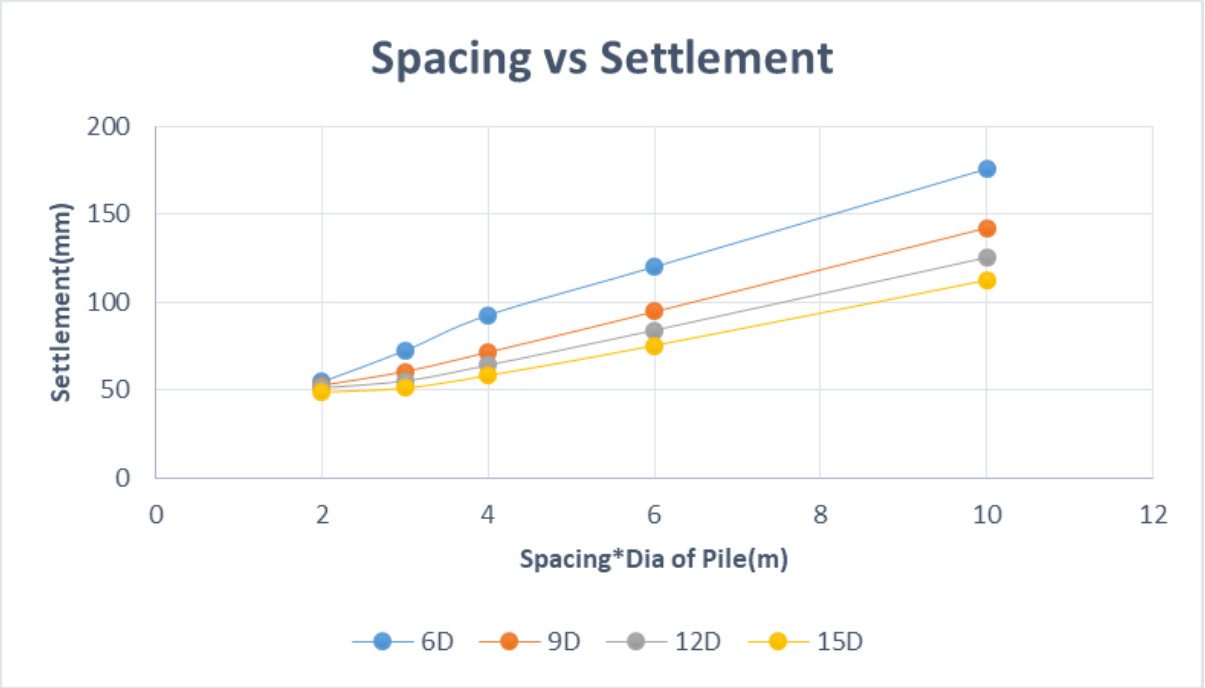


Figure 4.1 Spacing vs Settlement Graph.

From the graph, It is evident that as the spacing of piles is increased in CPRF, the resulting settlement also increases. For example, in depth 9D, when the spacing is increased from 2D to 3D the settlement increased by 7.86mm i.e 12.98% and when the spacing is increased from 6D to 10D the settlement increased by a huge amount of 47.68mm which is 50.43% of original value.

### 4.1.2 Variation in settlement of CPRF with Depth of Piles

For the determination of this variation, different piles of length 6D,9D,12D and 15D were used for each spacing and the resulting settlements were determined using Plaxis 3D software. Then a graph was plotted, plotting depth in X-axis and the resulting settlement in Y-axis. The resulting graph is shown below.

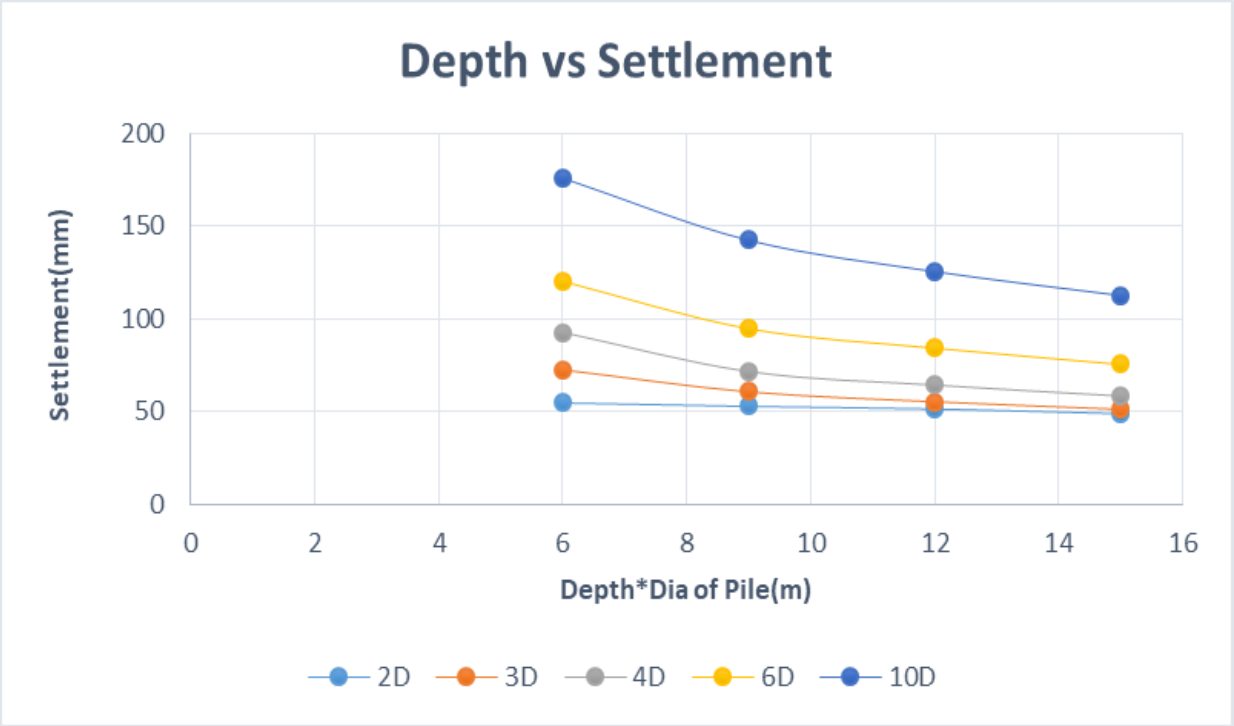


Figure 4.2 Depth vs Settlement graph.

From the graph, It is evident that the vertical displacement of CPRF declined due to the increase in length of the piles. However the efficiency in settlement is not the same for different pile length increases for different spacings. For example in case of 6D when the length of pile is increased from 6D to 9D the settlement was reduced by a value of 29.53mm which is approximately 23.8% meanwhile for the same spacing when the length of pile was increased from 12D to 15D the settlement was reduced unnoticeably by a value of only 8.73mm which is only 10.39% reduction of the original value.

### 4.2 Variation of Load sharing Mechanism:

The values of load shared by Piles and Rafts and the % load taken by piles as determined from Plaxis 3D software is shown in the tables below (All the loads are in kN):

| Spacing | 6D depth | | 9D depth | | 12D depth | | 15D depth | |
|---|---|---|---|---|---|---|---|---|
| | Pile Load | Raft Load | Pile Load | Raft Load | Pile Load | Raft Load | Pile Load | Raft Load |

| | | | | | | | | |
|---|---|---|---|---|---|---|---|---|
| 2D | 92378.88 | 37221.12 | 93726.72 | 35873.28 | 94672.8 | 34927.2 | 96526.08 | 33073.92 |
| 3D | 83371.68 | 46228.32 | 88957.44 | 40642.56 | 92093.76 | 37506.24 | 94698.72 | 34901.28 |
| 4D | 76140 | 53460 | 83669.76 | 45930.24 | 87078.24 | 42521.76 | 90188.64 | 39411.36 |
| 6D | 68351.04 | 61248.96 | 75492 | 54108 | 78809.76 | 50790.24 | 82088.64 | 47511.36 |
| 10D | 60108.48 | 69491.52 | 64968.48 | 64631.52 | 68052.96 | 61547.04 | 70800.48 | 58799.52 |

Table 4.2 Loads taken by piles and rafts in different depths and spacings

| Spacing | 6D depth | 9D depth | 12D depth | 15D depth |
|---|---|---|---|---|
| | % load on pile | % load on pile | % load on pile | % load on pile |
| 2D | 71.28 | 72.32 | 73.05 | 74.48 |
| 3D | 64.33 | 68.64 | 71.06 | 73.07 |
| 4D | 58.75 | 64.56 | 67.19 | 69.59 |
| 6D | 52.74 | 58.25 | 60.81 | 63.34 |
| 10D | 46.38 | 50.13 | 52.51 | 54.63 |

Table 4.3 % Load taken by Pile in CPRF at different depths and spacings

### 4.2.1 Variation in Load Sharing of CPRF with spacing of Piles:

For the determination of this variation, a constant surface load of 100 kN/m$^2$ was imposed on the CPRF and the Piles were Spaced at 2D,3D,4D,6D and 10D spacings. The values of total load taken by piles was determined from plaxis 3D software and a graph was plotted, plotting spacing in X-axis and % Load on pile in Y-axis. The graph is shown below.

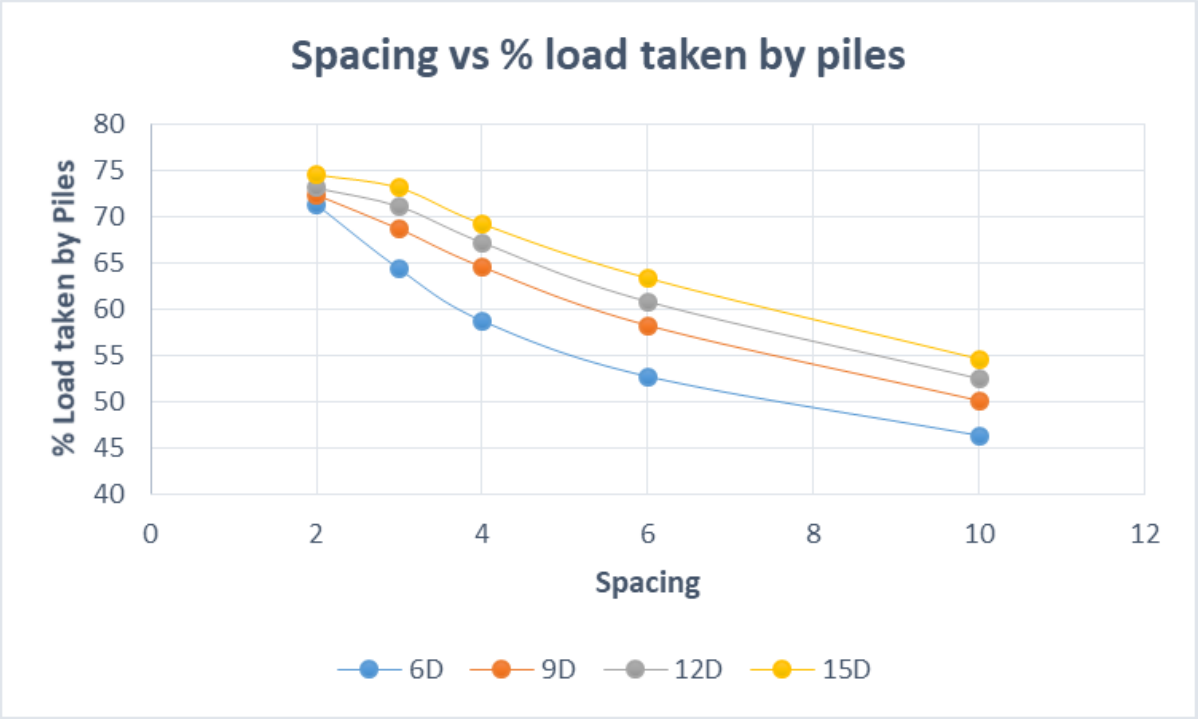


Figure 4.3 Spacing vs Load taken by Piles

From the graph it is evident that as the spacing of piles in the combined pile raft foundation increases or the number of piles decreases, the % load taken by the piles decreases as well.

For example, for length 6D of piles, when the spacing between piles is 2D, the % load taken by the piles is 71.28% and when the spacing of piles is increased to 10D, the % load taken by the piles reduces down to 46.38%.

### 4.2.2 Variation in Load sharing of CPRF with depth of Piles:

For the determination of this variation, a constant surface load of 100 kN/m2 was imposed on the CPRF and piles of lengths 6D,9D,12D and 15D were used for each pile spacing and the load sharing between the Raft and Piles was determined from plaxis 3D. After that a graph was plotted, plotting Depth in X-axis and % Load taken by piles in Y-axis. The graph is shown below:

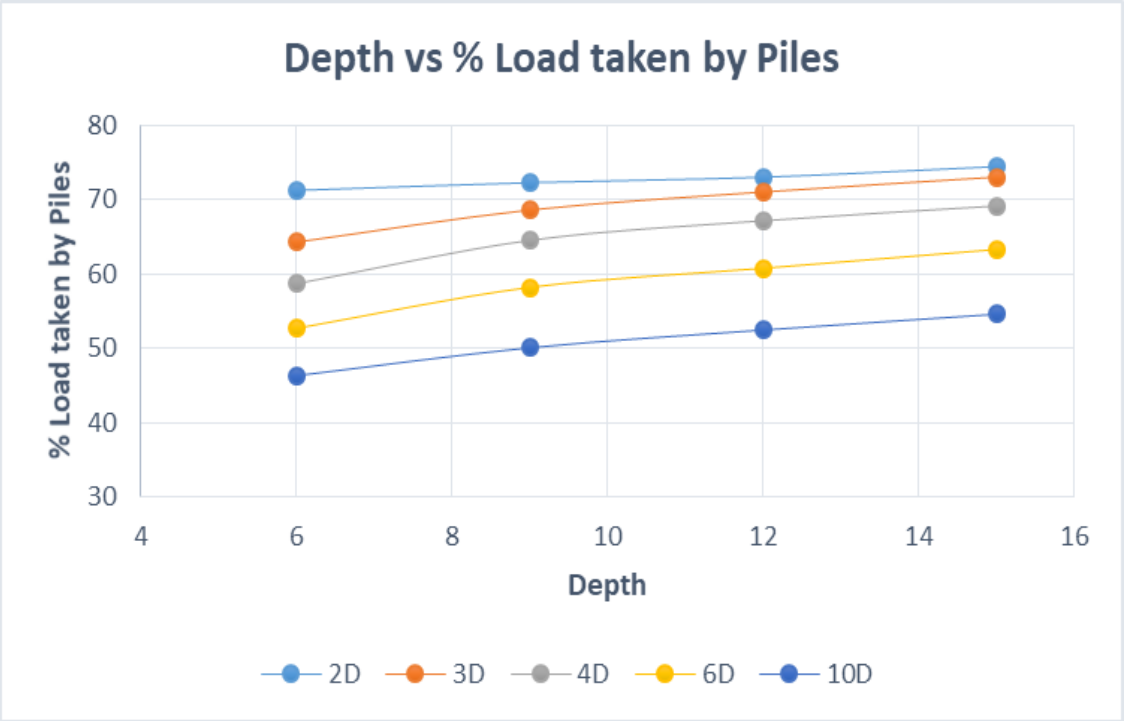


Figure 4.4 Depth vs Load taken by Piles

From the Graph, It is evident that as the depth of the piles is increased, the % load taken by the piles in CPRF increases as well. For example in 3D spacing, when the length of piles is 6D, the % load taken by piles is 64.33% and when the length is increased to 9D,12D and 15D the % load taken by pile also increases to 68.64%, 71.06% and 73.07% respectively.

### 4.3 Comparison between embedded beam method and volume pile method

For the comparison between embedded beam element method and volume pile method, a constant load of 100 kN/m2 was imposed on the CPRF. Piles of length 6D,9D,12D and 15D were used and the spacing was constant at 6D. Then the settlement was determined from plaxis 3D. After that a graph was plotted plotting, depth in X axis and settlement in Y axis. The resulting values of settlement and graph is shown below.

| Spacing = 6D | | |
|---|---|---|
| Depth | Settlement(mm) | |
| | Embedded Beam | Volume Pile |
| 6D | 124.07 | 120.13 |

| | | |
|---|---|---|
| 9D | 94.54 | 88.67 |
| 12D | 84.05 | 79.08 |
| 15D | 75.32 | 71.94 |

Table 4.4 Comparison in settlement between embedded beam and volume pile modelling

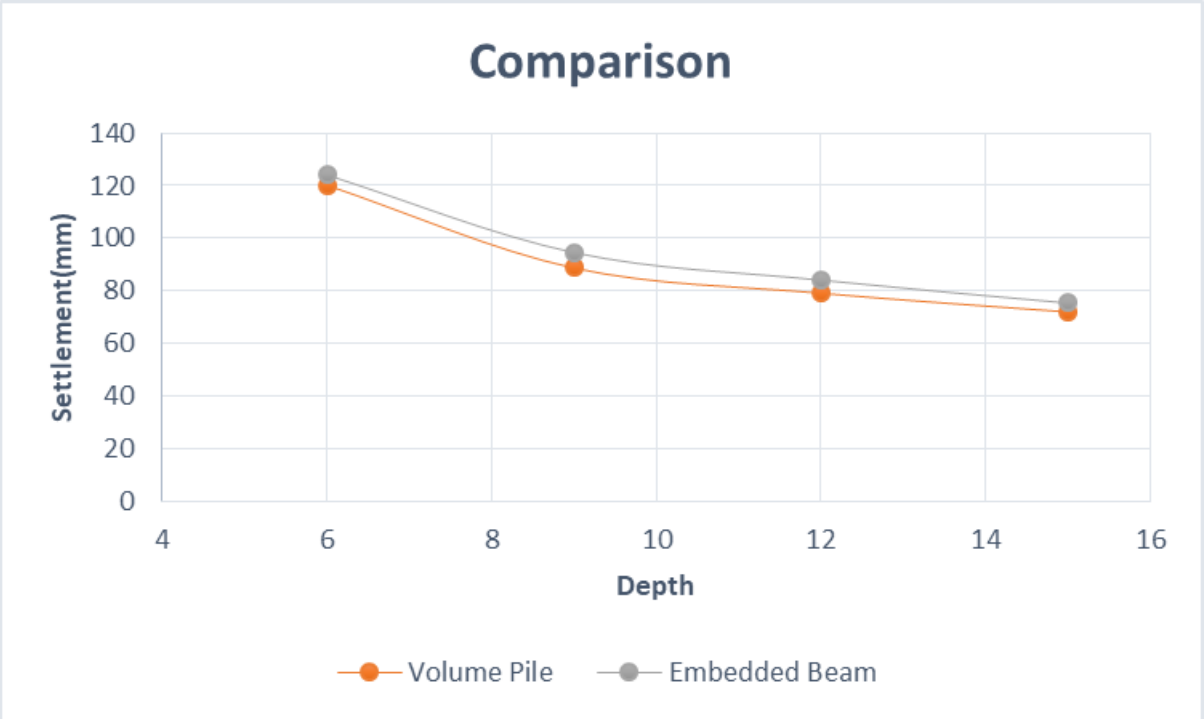


Figure 4.5 Comparison in settlement between embedded beam and volume pile modelling

From the data and graph, it can be seen that there is slight variation in settlement of CPRF when piles are modeled as embedded beam elements and volume elements. The Variations were pretty small and volume pile method is considered to be more accurate.

# Chapter 5: Design of Suitable Model

Out of all the analyzed CPRF models, one of the models was selected for design. The model was chosen on the basis of its suitability in terms settlement, load sharing and economy.

**a) Load Sharing:**

The load sharing of models from Plaxis-3D were compared with Kumar et al. 2016 paper and according to Kumar et al. for a combined pile raft foundation, the raft shares 23-31% of the total imposed load and the piles share the remaining 69-77% of the load. Manual calculation was also done to find the difference between calculated value and result from Plaxis 3D.

**b) Settlement:**

According to IS-1904(1966) for serviceability condition, the maximum allowable settlement of raft foundation used in buildings is 10 cm. The settlement of single deep foundation element or group thereof shall be estimated based on approved methods of analysis. The predicted settlement shall cause neither harmful distortion of, nor instability in, the structure, nor cause any element to be loaded beyond its capacity. (International Building Code, 2015).

On the basis of these conditions, we found CPRF with 4D spacing and 15D depth to be most suitable as it falls in the range of load sharing in Kumar et al. paper and its settlement is within allowable range as well.

| Result | Settlement | Remarks |
|---|---|---|
| Plaxis | 58.27mm | |
| Calculation | 61.78mm | 3.5mm diff from Plaxis |
| (NBC of India Vol. 1) Code | 0.1m | Within Range |

Table 5.1 Validation of Settlement of Selected Model

| Result | % Load Pile | % Load Raft | Remarks |
|---|---|---|---|
| Plaxis | 69.59 | 30.41 | 1.21% Skew |

| | | | |
|---|---|---|---|
| Calculation | 70.43 | 29.57 | |
| (Kumar et al. 2016) Paper | 69-77 | 23-31 | Within range |

Table 5.2 Validation of Load sharing of selected model

## 5.1 Layout of selected model:

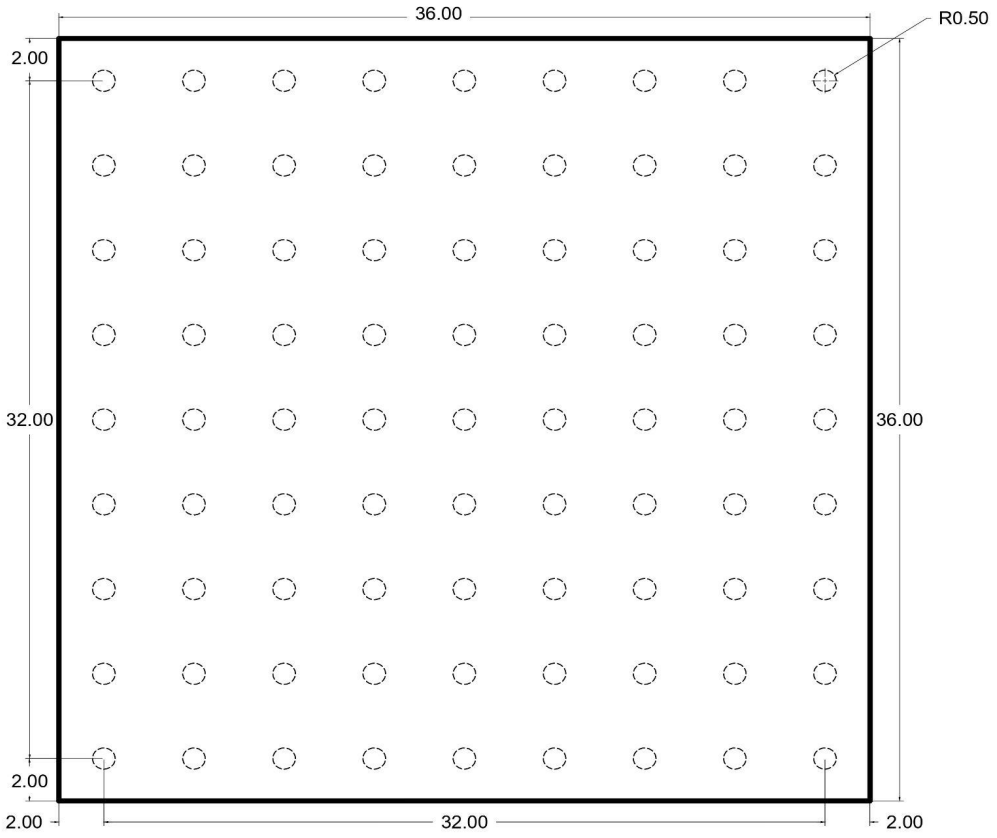


Figure 5.1 Top view of Selected Model

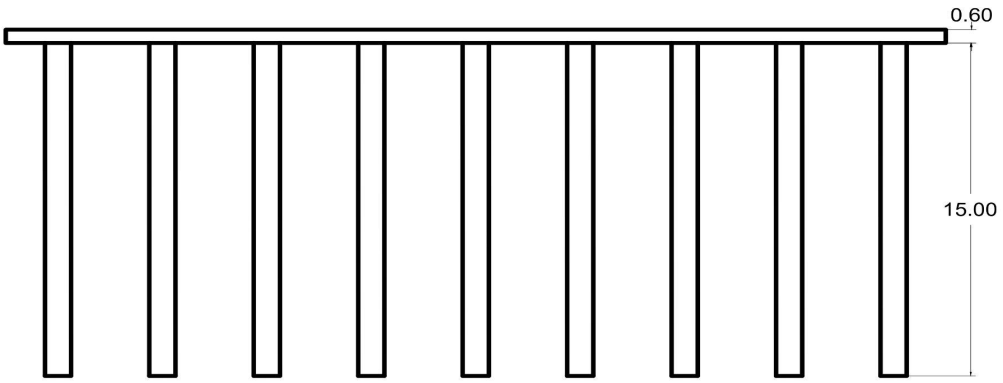


Figure 5.2 Side view of Selected Model

## 5.2 Final Parameters of Design:

The final parameters of our designed Combined pile raft foundation are listed below, the calculations are shown in Appendix-C:

| | |
|---|---|
| Length of Raft | 36 m |
| Width of Raft | 36 m |
| Thickness of Raft | 0.6 m |
| Length of Piles | 15 m |
| Diameter of Piles | 1 m |
| Spacing of Piles | 4m |
| Ultimate load Capacity of Raft (Qraft) | 788991.84 kN |
| Pile-Pile interaction factor (αpp) | 0.7227 |
| Ultimate load Capacity of Pile with pile-pile interaction factor (Qpile) | 189141.47 kN |
| Pile-Raft interaction factor (αpr) | 0.7862 |

| | |
|---|---|
| Raft-Pile interaction factor(αrp) | 0.539 |
| Bearing Capacity of CPRF (Qu=Qraft*αrp+ Qpile*αpr) | 573969.62 kN |
| Total Structural load (P) | 129600kN |
| Factor of Safety of structure (FOS=Qu/P) | 4.42 |
| Stiffness of Group of Piles | 374728.19 kN/m |
| Stiffness of Raft | 228952.1 kN/m |
| Stiffness of CPRF | 433886.01 kN/m |

Table 5.3 Parameters of design

# Chapter 6: Conclusion and Recommendations

## 6.1: Conclusion

The purpose of this research was to analyse the behaviour of combined pile raft foundation in the soil of Chakupat Area using Plaxis 3D software and to design a suitable Combined Pile Raft Foundation based on the settlement, load sharing and economy.

From the analysis, it was found that as the spacing and number of piles is increased, the settlement of the CPRF increases as well. And when the length of the piles is increased for the same spacing the resulting settlement reduces. It was also found that as the spacing of piles/number of piles is decreased, the % load taken by piles in CPRF decreases as well and as the length of the piles is increased, the % load taken by the piles increases as well. A comparison in settlement while modelling piles as volume element and embedded beam elements was also done and it was found that there was slight variation in result.

Considering Load sharing, Settlement, Economy and Soil structure analysis a foundation was designed with raft thickness 0.6m, Pile length 15m, diameter 1m and spacing of 4m. The percentage load sharing of the plies and raft were found to be 69.59% and 30.41% respectively which were found to be within allowable range. The settlement of the CPRF was found to be 58.27 mm which was also within allowable range. The bearing capacity of the foundation was found to be 573969.62 kN and a factor of safety of 4.42 was achieved.

Hence CPRF seemed a reliable design approach for building foundations of high rise buildings in areas where the soil contains high amounts of sand, silt and low amounts of clay and in areas where water table is relatively higher. However, the foundation engineers should focus on finding optimum thickness of raft, optimum length, diameter and spacing of piles for economical design. If not, the overall cost of the foundation will be costly.

### 6.2: Recommendations

Due to constraints of time, money and equipment, some assumptions were made during the project study. But the assumptions were made by doing a thorough study of different related articles and papers on CPRF.

Following are the recommendations made for further studies:

1. Our study primarily focuses on axial loads on the foundation. Lateral and inclined loads can also be considered for more accurate results.
2. The effects of seismic loads and dynamic loading conditions can be considered for more realistic behaviour of foundation.
3. The variation of ground water table can be further studied in depth.
4. Instead of Direct shear test, triaxial test can be done for more accurate value of shear strength parameters.
5. Different soil and loading conditions will help in understanding the behaviour of the foundation system and its response to different stresses.
6. Analysing failure causes of CPRF to understand the causes and mechanism of failure can also be researched.

.

## References


Azhar, S., Patidar, A., & Jaurker, S. (2020). Parametric Study of Piled Raft Foundation for High Rise Buildings. *International Journal of Engineering Research & Technology*, *9*(12), 548-555..

Basile, F. (2015). Non-linear analysis of vertically loaded piled rafts. *Computers and Geotechnics*, *63*, 73-82.

Chandiwala, A. K., & Vasanwala, D. S. (2018). A Parametric Study on Behaviour of Piled Raft Foundation-Structure Interaction Effects on Seismic Performance of Multi-Story Regular RC MRF Building. *International Journal of Civil Engineering and Technology*, *9*(7), 558-567.

Deb, P., & Pal, S. K. (2019). Analysis of load sharing response and prediction of interaction behaviour in piled raft foundation. *Arabian Journal for Science and Engineering*, *44*, 8527-8543.

Elwakil, A. Z., & Azzam, W. R. (2016). Experimental and numerical study of piled raft system. *Alexandria Engineering Journal*, *55*(1), 547-560.

El-Garhy, B., Galil, A. A., Youssef, A. F., & Raia, M. A. (2013). Behavior of raft on settlement reducing piles: Experimental model study. *Journal of Rock Mechanics and Geotechnical Engineering*, *5*(5), 389-399.

Fraser, R. A., & Wardle, L. J. (1976). Numerical analysis of rectangular rafts on layered foundations. *Geotechnique*, *26*(4), 613-630.

Fleming, K., Weltman, A., Randolph, K. & Elson, K. (1992). "Piling engineering." Taylor & Francis.

Gupta, S.C. (1997). "Design of Raft Foundations." New Age International Limited.

Hooper, J. A. (1973). Observations on the behaviour of a pile-raft foundation on London Clay. *Proceedings of the institution of civil engineers*, *55*(4), 855-877

Kitiyodom, P., & Matsumoto, T. (2003). A simplified analysis method for piled raft foundations in non-homogeneous soils. *International Journal for Numerical and Analytical Methods in Geomechanics*, *27*(2), 85-109.

Kim, K. N., Lee, S. H., Kim, K. S., Chung, C. K., Kim, M. M., & Lee, H. S. (2001). Optimal pile arrangement for minimizing differential settlements in piled raft foundations. *Computers and Geotechnics*, *28*(4), 235-253.

Kumar, A., Choudhury, D., & Katzenbach, R. (2016). Effect of earthquake on combined pile–raft foundation. *International Journal of Geomechanics*, *16*(5), 04016013.

Kumar, A. and Choudhury, D. (2018), "Development of new prediction model for capacity of combined pile-raft Foundations." *Journal on Computers and Geotechnics*, No. 97, pp 62-68.

Lee, J., Park, D., & Choi, K. (2014). Analysis of load sharing behavior for piled rafts using normalized load response model. *Computers and Geotechnics*, *57*, 65-74.

Luo, R., Yang, M., & Li, W. (2018). Normalized settlement of piled raft in homogeneous clay. *Computers and Geotechnics*, *103*, 165-178.

Meyerhof, G. G. (1963). "Some recent research on the bearing capacity of foundations." *Canada Geotechnical Journal 1(1).* 16-23.

Nguyen, D. D. C., Jo, S. B., & Kim, D. S. (2013). Design method of piled-raft foundations under vertical load considering interaction effects. *Computers and Geotechnics*, *47*, 16-27.

Poulos, H. G., & Davis, E. H. (1980). *Pile foundation analysis and design* (Vol. 397). New York: Wiley.

Poulos, H. G. (2001). Piled raft foundations: design and applications. *Geotechnique*, *51*(2), 95-113

Poulos, H. G., Small, J. C., & Chow, H. (2011). Piled raft foundations for tall buildings. *Geotechnical Engineering Journal of the SEAGS & AGSSEA*, *42*(2), 78-84.

Prakoso, W. A., & Kulhawy, F. H. (2001). Contribution to piled raft foundation design. *Journal of Geotechnical and Geoenvironmental Engineering*, *127*(1), 17-24.

Randolph, M. F. (1994) "Design methods for pile groups and piled rafts". 13th International Conference for Soil Mechanics and Foundation Engineering, New Delhi, 5, pp. 61-82.

Sinha, A., & Hanna, A. M. (2017). 3D numerical model for piled raft foundation. *International Journal of Geomechanics*, *17*(2), 04016055.

Srilakshmi, G., & Darshan Moudgalya, N. S. (2013). Analysis of piled raft foundation using finite element method. *International Journal of Engineering Research and Science & Technology*, *2*(3), 89-96.

Tradigo, F., Pisanò, F., & di Prisco, C. (2016). On the use of embedded pile elements for the numerical analysis of disconnected piled rafts. *Computers and Geotechnics*, *72*, 89-99.

Terzaghi, K. and Peck, R.B. (1967). "Soil Mechanics in Engineering Practice." John Wiley and Sons New York

Tschuchnigg, F., & Schweiger, H. F. (2015). The embedded pile concept–Verification of an efficient tool for modelling complex deep foundations. *Computers and Geotechnics*, *63*, 244-254.

Unsever, Y. S., Matsumoto, T., & Özkan, M. Y. (2015). Numerical analyses of load tests on model foundations in dry sand. *Computers and Geotechnics*, *63*, 255-266.

# APPENDIX - A

## Soil Parameters from Laboratory

**A-1 Determination of Water Content of soil sample**

| Container No. | 1015 | 1046 | 1050 |
|---|---|---|---|
| Wt of empty Container | 21.27 gm | 10.10 gm | 15.48 gm |
| Wt of container with soil | 77.43 gm | 68.16 gm | 79.49 gm |
| Wt of container with oven dried soil | 64.30 gm | 54.61 gm | 64.69 gmq |
| Wt of water in the soil | 13.13 gm | 13.55 gm | 14.8 gm |
| Wt of solids | 43.03 gm | 44.51 gm | 49.21 gm |
| Water Content (%) | 30.51 | 30.44 | 30.07 |
| Average Water Content | 30.34% | | |

**A-2 Determination of Specific Gravity by Density Bottle Method**

| Wt of bottle with stopper M1 (gm) | 56.9 gm |
|---|---|
| Wt of bottle with dry sand M2 (gm) | 66.93 gm |
| Wt of bottle, soil and water M3 (gm) | 162.07 gm |
| Wt of bottle filled with water M4 (gm) | 156.10 gm |
| M2-M1 (gm) | 10.03 |
| M3-M4 (gm) | 5.97 |
| Specific gravity = (M2-M1)/((M2-M1)-(M3-M4)) | 2.469 |

**A-3 Determination of Wet and Dry density by Core Cutter Method**

| | |
|---|---|
| Internal diameter of cutter (mm) | 100 mm |
| Internal height of cutter (mm) | 129.75 mm |
| Mass of empty core cutter (gm) | 1130 gm |
| Mass of core cutter with soil (gm) | 2942.89 gm |
| Mass of wet soil (gm) | 1812.89 gm |
| Volume of cutter (ml) | 1019.05 ml |
| Wet density | 1.779 g/ml |
| Water content (%) | 30.34 |
| Dry density | 1.365 g/ml |

**A-4 Determination of Liquid Limit of Soil**

| S.N | Observations | Sample 1 | Sample 2 | Sample 3 |
|---|---|---|---|---|
| 1 | No. of blows(N) | 19 | 23 | 31 |
| 2 | Can No. | 1029 | 1011 | 1042 |
| 3 | Mass of empty can (M1) gm | 25.52 | 7.07 | 6.63 |
| 4 | Mass of can + Wet soil (M2) gm | 101.55 | 87.83 | 84.78 |
| 5 | Mass of can + Dry soil (M3) gm | 80.77 | 66.3 | 64.38 |
| 6 | Mass of water = M2-M3 gm | 20.78 | 21.53 | 20.4 |
| 7 | Mass of dry soil = M3-M1 gm | 55.25 | 59.23 | 57.75 |
| 8 | Water Content % | 37.611 | 36.350 | 35.325 |

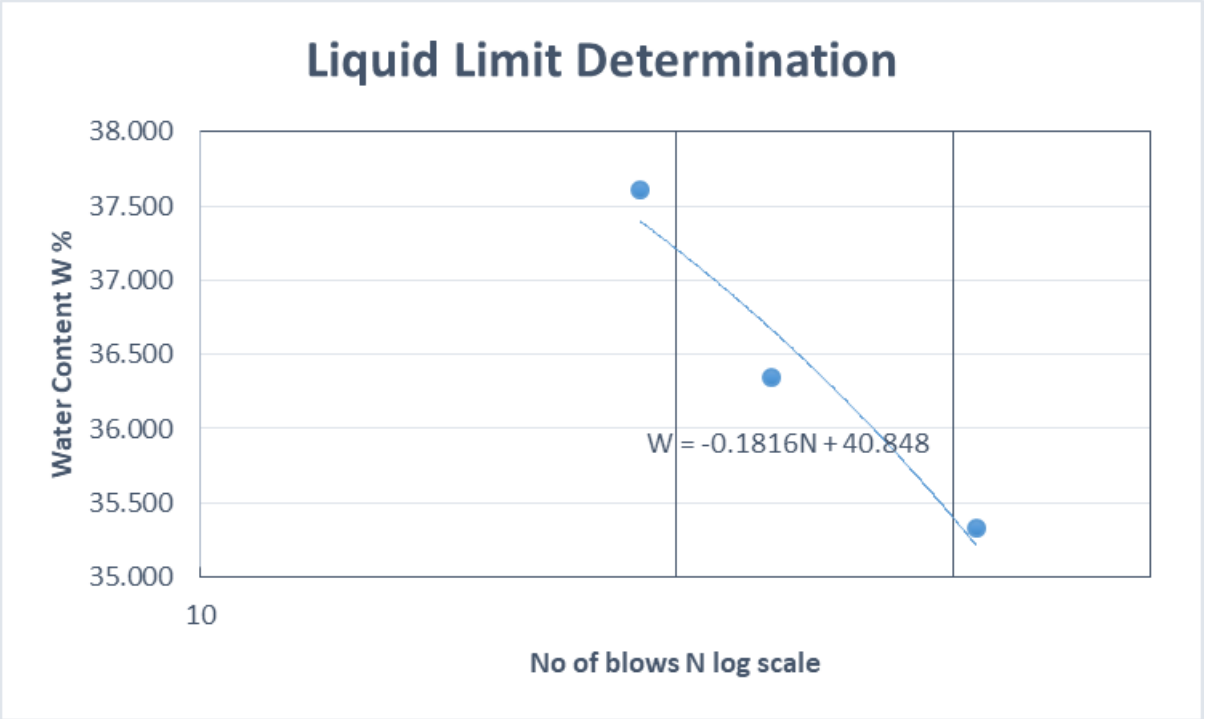


Water content corresponding to 25 Blows= 36.328 %

Hence, Liquid Limit= 36.328%

**A-5 Determination of Plastic Limit of Soil**

| S.N | Observations | Sample 1 | Sample 2 | Sample 3 |
|---|---|---|---|---|
| 1 | Can No. | 1012 | 1000 | 1048 |
| 2 | Mass of empty can (M1) gm | 6.87 | 10.37 | 8.58 |
| 3 | Mass of can + Wet soil (M2) gm | 17.84 | 21.31 | 19.36 |
| 4 | Mass of can + Dry soil (M3) gm | 15.34 | 18.89 | 16.89 |
| 5 | Mass of water = M2-M3 gm | 2.5 | 2.42 | 2.47 |
| 6 | Mass of dry soil = M3-M1 gm | 8.47 | 8.52 | 8.31 |
| 7 | Water Content % | 29.516 | 28.404 | 29.723 |
| | Average Plastic Limit = | 29.214 | | |

**A-6 Gradation of the Soil Sample**

**A-6.1 Sieve Analysis Calculation**

Wt of Empty Pan= 845 gm

Wt of Pan of Soil= 1400 gm

Wt of Soil= 555 gm

| IS sieve(mm) | Wt of empty sieve(gm) | Wt of sieve with soil(gm) | Soil Retained(gm) | Percentage Retained | Cumulative % Retained | % Finer |
|---|---|---|---|---|---|---|
| 2.36 | 361.55 | 361.9 | 0.35 | 0.06 | 0.06 | 99.94 |
| 1.18 | 372.65 | 378.97 | 6.32 | 1.14 | 1.20 | 98.80 |
| 0.6 | 205.1 | 209.14 | 4.04 | 0.73 | 1.93 | 98.07 |
| 0.5 | 314.19 | 317.5 | 3.31 | 0.60 | 2.53 | 97.47 |
| 0.425 | 201.31 | 202.98 | 1.67 | 0.30 | 2.83 | 97.17 |
| 0.3 | 336.14 | 346.3 | 10.16 | 1.83 | 4.66 | 95.34 |
| 0.15 | 304.51 | 338.86 | 34.35 | 6.19 | 10.85 | 89.15 |
| 0.075 | 302.15 | 356.22 | 54.07 | 9.74 | 20.59 | 79.41 |
| Pan | 284.04 | 284.18 | 440.53 | 79.41 | 100 | 0 |
| | | Sum | 554.8 | 100 | | |

**A-6.2 Hydrometer Analysis Calculation**

| Wt of soil =50 gm | Dispersing Agent =$(NaPO_3)_6$ | Soil =5 gm | Specific Gravity of Solids =2.469 |
|---|---|---|---|

| | | |
|---|---|---|
| Temp = 15°C | Amount = 5 gm | Passing 0.075mm = 79.41 % |
| γw=1.0015 | Zero Correction = -0.0035 | |

| Time (min) | Actual hyd. Reading | Temp °C | Corrected Hyd. Reading | Hyd. Reading in water | R-Rw | K1 | % Finer K1*(R-Rw) | Correction for meniscus and temp | Effective Length L (cm) | L/t | K2 | Diameter D mm K2*sqrt(L/t) | Actual % finer |
|---|---|---|---|---|---|---|---|---|---|---|---|---|---|
| | | | | | | | | | | | | 0.0750 | 79.41 |
| 0.5 | 1.023 | 15 | 19.5 | 1.5 | 18 | 3.496 | 62.93 | 17.84 | 10.2 | 20.4 | 0.0139 | 0.0629 | 49.97 |
| 1 | 1.023 | 15 | 19.5 | 1.5 | 18 | 3.496 | 62.93 | 17.84 | 10.2 | 10.2 | 0.0139 | 0.0444 | 49.97 |
| 2 | 1.022 | 15 | 18.5 | 1.5 | 17 | 3.496 | 59.43 | 16.84 | 10.5 | 5.25 | 0.0139 | 0.0319 | 47.19 |
| 3 | 1.021 | 15 | 17.5 | 1.5 | 16 | 3.496 | 55.93 | 15.84 | 10.7 | 3.57 | 0.0139 | 0.0263 | 44.42 |
| 4 | 1.02 | 15 | 16.5 | 1.5 | 15 | 3.496 | 52.44 | 14.84 | 11 | 2.75 | 0.0139 | 0.0231 | 41.64 |
| 8 | 1.018 | 15 | 14.5 | 1.5 | 13 | 3.496 | 45.45 | 12.84 | 11.5 | 1.44 | 0.0139 | 0.0167 | 36.09 |
| 15 | 1.016 | 15 | 12.5 | 1.5 | 11 | 3.496 | 38.46 | 10.84 | 12.1 | 0.81 | 0.0139 | 0.0125 | 30.54 |
| 30 | 1.014 | 15 | 10.5 | 1.5 | 9 | 3.496 | 31.46 | 8.84 | 12.6 | 0.42 | 0.0139 | 0.0090 | 24.99 |
| 60 | 1.012 | 15 | 8.5 | 1.5 | 7 | 3.496 | 24.4 | 6.84 | 13.1 | 0.22 | 0.013 | 0.006 | 19.4 |

| | | | | | | | | | | | | | |
|---|---|---|---|---|---|---|---|---|---|---|---|---|---|
| | | | | | | | 7 | | | | 9 | 5 | 3 |
| 120 | 1.01 | 15 | 6.5 | 1.5 | 5 | 3.496 | 17.48 | 4.84 | 13.7 | 0.11 | 0.0139 | 0.0047 | 13.88 |
| 240 | 1.009 | 15 | 5.5 | 1.5 | 4 | 3.496 | 13.98 | 3.84 | 13.9 | 0.06 | 0.0139 | 0.0033 | 11.10 |
| 1440 | 1.008 | 15 | 4.5 | 1.5 | 3 | 3.496 | 10.49 | 2.84 | 14.2 | 0.01 | 0.0139 | 0.0014 | 8.33 |

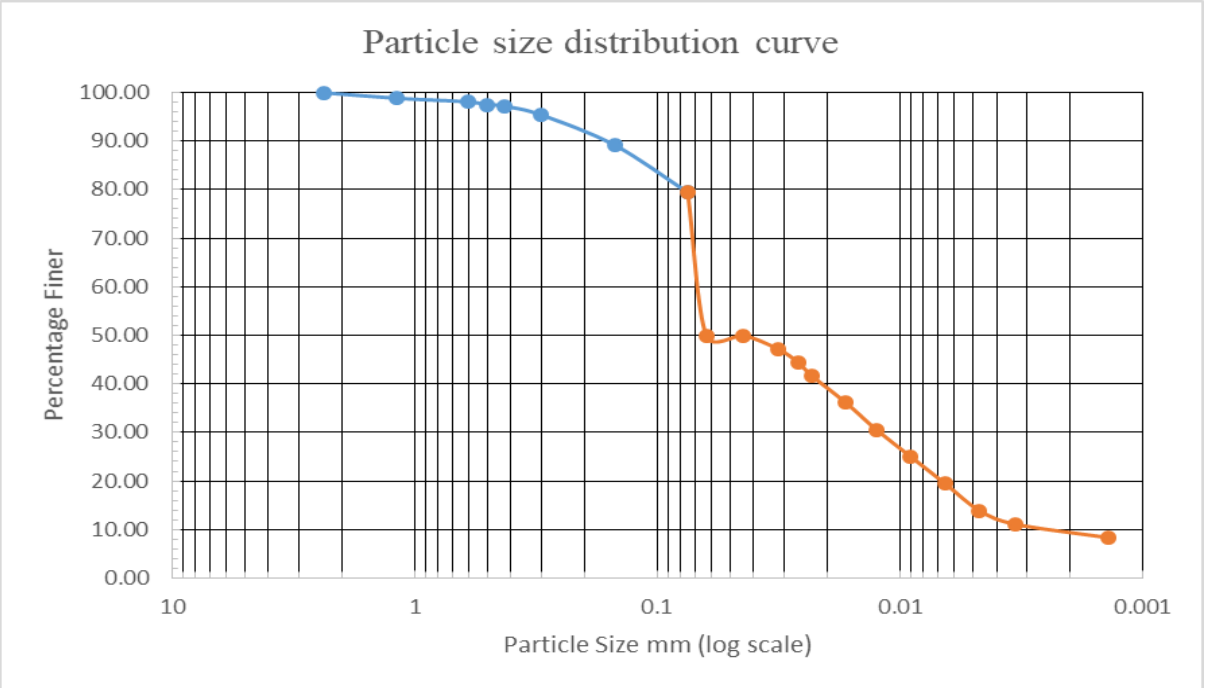


Figure. Particle size distribution curve

From the Particle Size Distribution Curve:

| | |
|---|---|
| % Gravel | 0.40% |
| % of Sand | 49.70% |
| % of Silt | 40.60% |
| % of Clay | 9.30% |

**A-7 Unconfined Compression Test**

Diameter of specimen= 38mm

Length of Specimen= 75mm

Load Factor= 0.14kg/div

| S.N | Dial Gauge | LC= 0.01 mm | Deformation(dL) (cm) | Strain(ε) | Proving Ring Reading | Load P(kg) | Corrected Area | Compressive Stress σ=P/A (kg/cm²) | Compressive Stress(kN/m²) | % Strain |
|---|---|---|---|---|---|---|---|---|---|---|
| 1 | 0 | 0.01 | 0 | 0 | 0 | 0 | 11.34 | 0.000 | 0 | 0 |
| 2 | 20 | 0.01 | 0.02 | 0.0027 | 10 | 1.4 | 11.37 | 0.12 | 12.07 | 0.27 |
| 3 | 40 | 0.01 | 0.04 | 0.0053 | 18 | 2.52 | 11.40 | 0.22 | 21.67 | 0.53 |
| 4 | 60 | 0.01 | 0.06 | 0.0080 | 25 | 3.5 | 11.43 | 0.31 | 30.02 | 0.80 |
| 5 | 80 | 0.01 | 0.08 | 0.0107 | 32 | 4.48 | 11.46 | 0.39 | 38.33 | 1.07 |
| 6 | 100 | 0.01 | 0.1 | 0.0133 | 37 | 5.18 | 11.49 | 0.45 | 44.19 | 1.33 |
| 7 | 120 | 0.01 | 0.12 | 0.0160 | 40 | 5.6 | 11.53 | 0.49 | 47.65 | 1.60 |
| 8 | 140 | 0.01 | 0.14 | 0.0187 | 43 | 6.02 | 11.56 | 0.52 | 51.08 | 1.87 |
| 9 | 160 | 0.01 | 0.16 | 0.0213 | 45 | 6.3 | 11.59 | 0.54 | 53.31 | 2.13 |
| 10 | 180 | 0.01 | 0.18 | 0.0240 | 48 | 6.72 | 11.62 | 0.58 | 56.71 | 2.40 |
| 11 | 200 | 0.01 | 0.2 | 0.0267 | 48 | 6.72 | 11.65 | 0.58 | 56.56 | 2.67 |
| 12 | 220 | 0.01 | 0.22 | 0.0293 | 33 | 4.62 | 11.68 | 0.40 | 38.78 | 2.93 |
| 13 | 240 | 0.01 | 0.24 | 0.0320 | 20 | 2.8 | 11.72 | 0.24 | 23.44 | 3.20 |
| 14 | 260 | 0.01 | 0.26 | 0.0347 | 14 | 1.96 | 11.75 | 0.17 | 16.36 | 3.47 |
| 15 | 280 | 0.01 | 0.28 | 0.0373 | 11 | 1.54 | 11.78 | 0.13 | 12.82 | 3.73 |

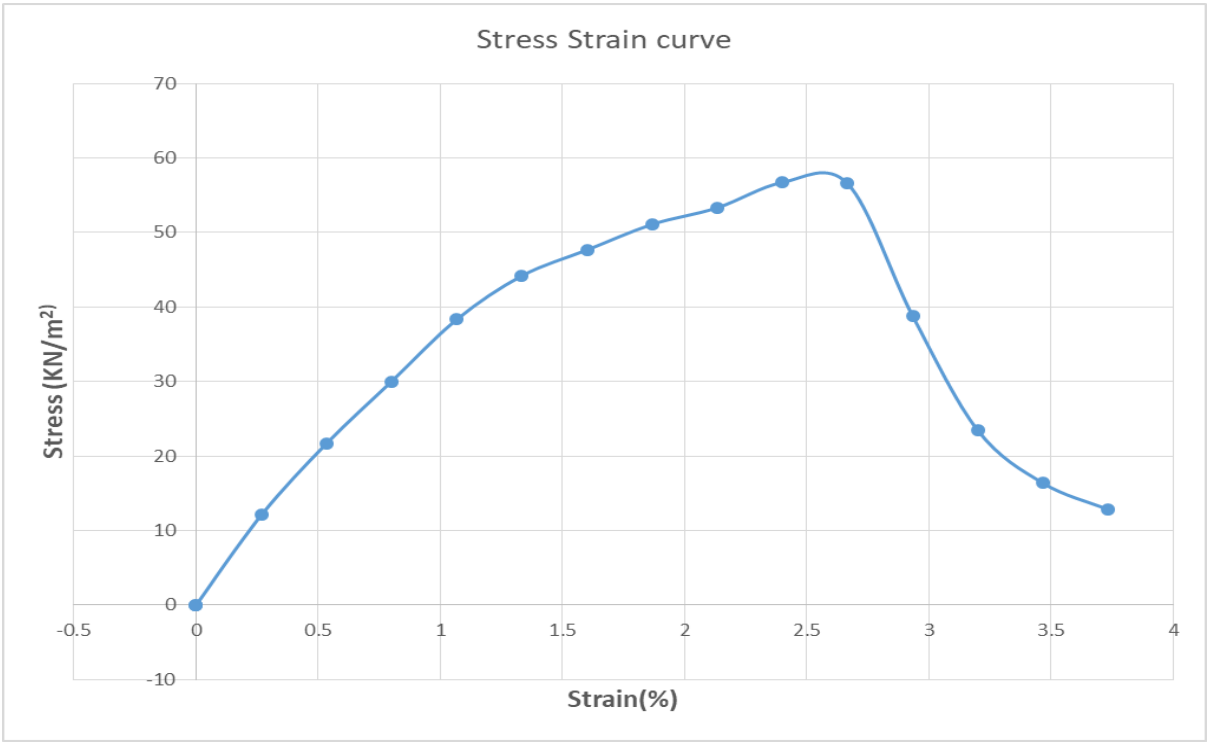


Figure. Stress vs Strain Curve

From the stress strain curve,

Modulus of Elasticity of Soil= 3314.651 kpa

And, Unconfined Compressive Strength= 56.713 kpa

**A-8 Direct Shear Test**

Load factor = 0.17 kg/div

Area of specimen = 5.081*5.081 = 25.817 cm²

Mass of glass+mould+soil= 394 gm

**Trial I (2 kg) Normal stress =7.75 kpa**

| S.N | Deflection dial gauge reading | LC=0.01 mm | Displacement(mm) | Load dial gauge reading | Load (kg) | Shear Stress( kpa) |
|---|---|---|---|---|---|---|

| | | | | | | |
|---|---|---|---|---|---|---|
| 1 | 20 | 0.01 | 0.2 | 10 | 1.7 | 6.46 |
| 2 | 40 | 0.01 | 0.4 | 15 | 2.55 | 9.69 |
| 3 | 60 | 0.01 | 0.6 | 19 | 3.23 | 12.27 |
| 4 | 80 | 0.01 | 0.8 | 22 | 3.74 | 14.21 |
| 5 | 100 | 0.01 | 1 | 25 | 4.25 | 16.14 |
| 6 | 120 | 0.01 | 1.2 | 26 | 4.42 | 16.79 |
| 7 | 140 | 0.01 | 1.4 | 27 | 4.59 | 17.44 |
| 8 | 160 | 0.01 | 1.6 | 27 | 4.59 | 17.44 |

**Trial II (4 kg) Normal stress = 15.31 kpa**

| S.N | Deflection dial gauge reading | LC=0.01 mm | Displacement( mm) | Load dial gauge reading | Load (kg) | Shear Stress( kpa) |
|---|---|---|---|---|---|---|
| 1 | 20 | 0.01 | 0.2 | 10 | 1.7 | 6.46 |
| 2 | 40 | 0.01 | 0.4 | 15 | 2.55 | 9.69 |
| 3 | 60 | 0.01 | 0.6 | 18 | 3.06 | 11.62 |
| 4 | 80 | 0.01 | 0.8 | 20 | 3.4 | 12.92 |
| 5 | 100 | 0.01 | 1 | 23 | 3.91 | 14.85 |
| 6 | 120 | 0.01 | 1.2 | 25 | 4.25 | 16.14 |
| 7 | 140 | 0.01 | 1.4 | 26 | 4.42 | 16.79 |
| 8 | 160 | 0.01 | 1.6 | 27 | 4.59 | 17.44 |
| 9 | 180 | 0.01 | 1.8 | 28 | 4.76 | 18.08 |
| 10 | 200 | 0.01 | 2 | 30 | 5.1 | 19.37 |
| 11 | 220 | 0.01 | 2.2 | 31 | 5.27 | 20.02 |
| 12 | 240 | 0.01 | 2.4 | 32 | 5.44 | 20.66 |

| | | | | | | |
|---|---|---|---|---|---|---|
| 13 | 260 | 0.01 | 2.6 | 32 | 5.44 | 20.66 |
| 14 | 280 | 0.01 | 2.8 | 33 | 5.61 | 21.31 |
| 15 | 300 | 0.01 | 3 | 33 | 5.61 | 21.31 |

**Trial III (8kg) Normal Stress = 30.50 kpa**

| S.N | Deflection dial gauge reading | LC=0.01 mm | Displacement(mm) | Load dial gauge reading | Load (kg) | Shear Stress( kpa) |
|---|---|---|---|---|---|---|
| 1 | 20 | 0.01 | 0.2 | 15 | 2.55 | 9.69 |
| 2 | 40 | 0.01 | 0.4 | 20 | 3.4 | 12.92 |
| 3 | 60 | 0.01 | 0.6 | 24 | 4.08 | 15.50 |
| 4 | 80 | 0.01 | 0.8 | 27 | 4.59 | 17.44 |
| 5 | 100 | 0.01 | 1 | 29 | 4.93 | 18.73 |
| 6 | 120 | 0.01 | 1.2 | 30 | 5.1 | 19.37 |
| 7 | 140 | 0.01 | 1.4 | 32 | 5.44 | 20.66 |
| 8 | 160 | 0.01 | 1.6 | 33 | 5.61 | 21.31 |
| 9 | 180 | 0.01 | 1.8 | 34 | 5.78 | 21.96 |
| 10 | 200 | 0.01 | 2 | 35 | 5.95 | 22.60 |
| 11 | 220 | 0.01 | 2.2 | 35 | 5.95 | 22.60 |
| 12 | 240 | 0.01 | 2.4 | 35 | 5.95 | 22.60 |
| 13 | 260 | 0.01 | 2.6 | 36 | 6.12 | 23.25 |
| 14 | 280 | 0.01 | 2.8 | 37 | 6.29 | 23.89 |
| 15 | 300 | 0.01 | 3 | 38 | 6.46 | 24.54 |
| 16 | 320 | 0.01 | 3.2 | 40 | 6.8 | 25.83 |

| | | | | | | |
|---|---|---|---|---|---|---|
| 17 | 340 | 0.01 | 3.4 | 40 | 6.8 | 25.83 |
| 18 | 360 | 0.01 | 3.6 | 40 | 6.8 | 25.83 |
| 19 | 380 | 0.01 | 3.8 | 41 | 6.97 | 26.48 |
| 20 | 400 | 0.01 | 4 | 42 | 7.14 | 27.12 |
| 21 | 420 | 0.01 | 4.2 | 43 | 7.31 | 27.77 |
| 22 | 440 | 0.01 | 4.4 | 44 | 7.48 | 28.41 |
| 23 | 460 | 0.01 | 4.6 | 44 | 7.48 | 28.41 |
| 24 | 480 | 0.01 | 4.8 | 44 | 7.48 | 28.41 |

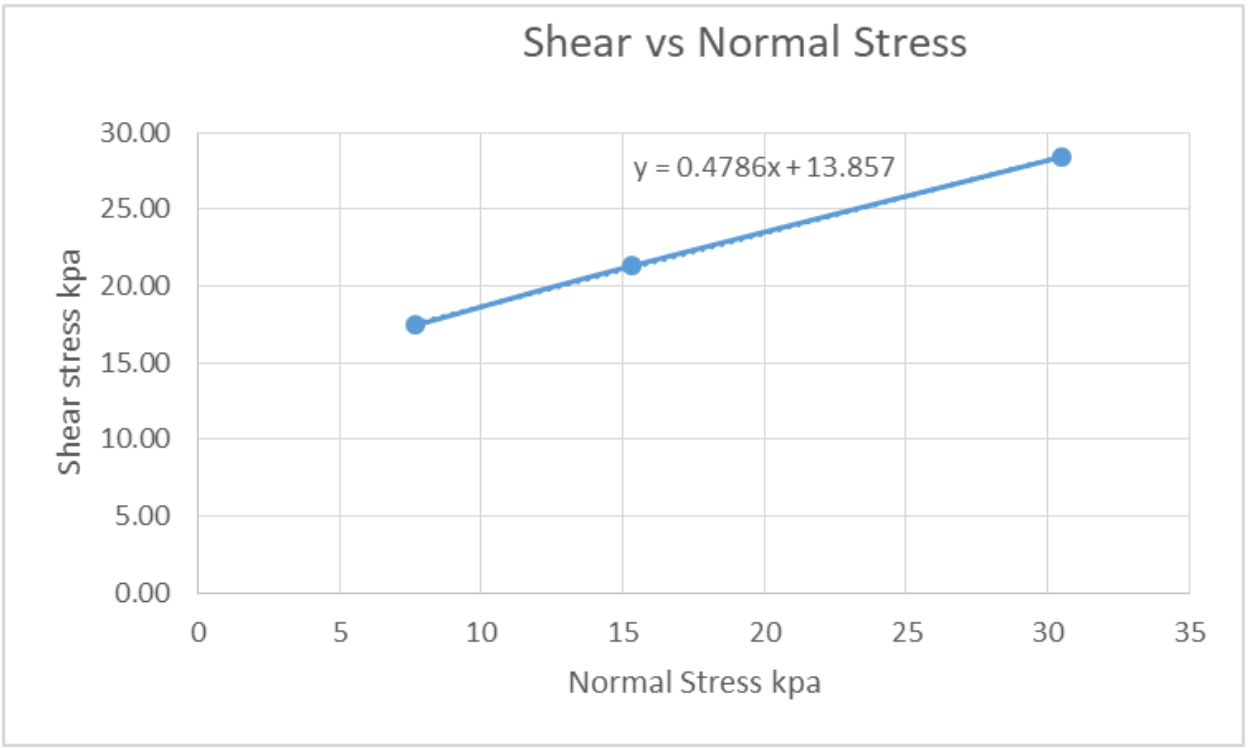


Figure : Normal Stress vs Shear Stress Curve

From the Normal Stress vs Shear Stress Curve,

| Normal Stress | Shear Stress |
|---|---|
| (kPa) | (kPa) |
| 7.65 | 17.44 |
| 15.31 | 21.31 |
| 30.5 | 28.41 |

| | |
|---|---|
| Cohesion (kPa) | 13.86 |
| Friction Angle | 25.58 |

# APPENDIX-B

## Classification of Soil

**B-1 Textural classification of Soil**

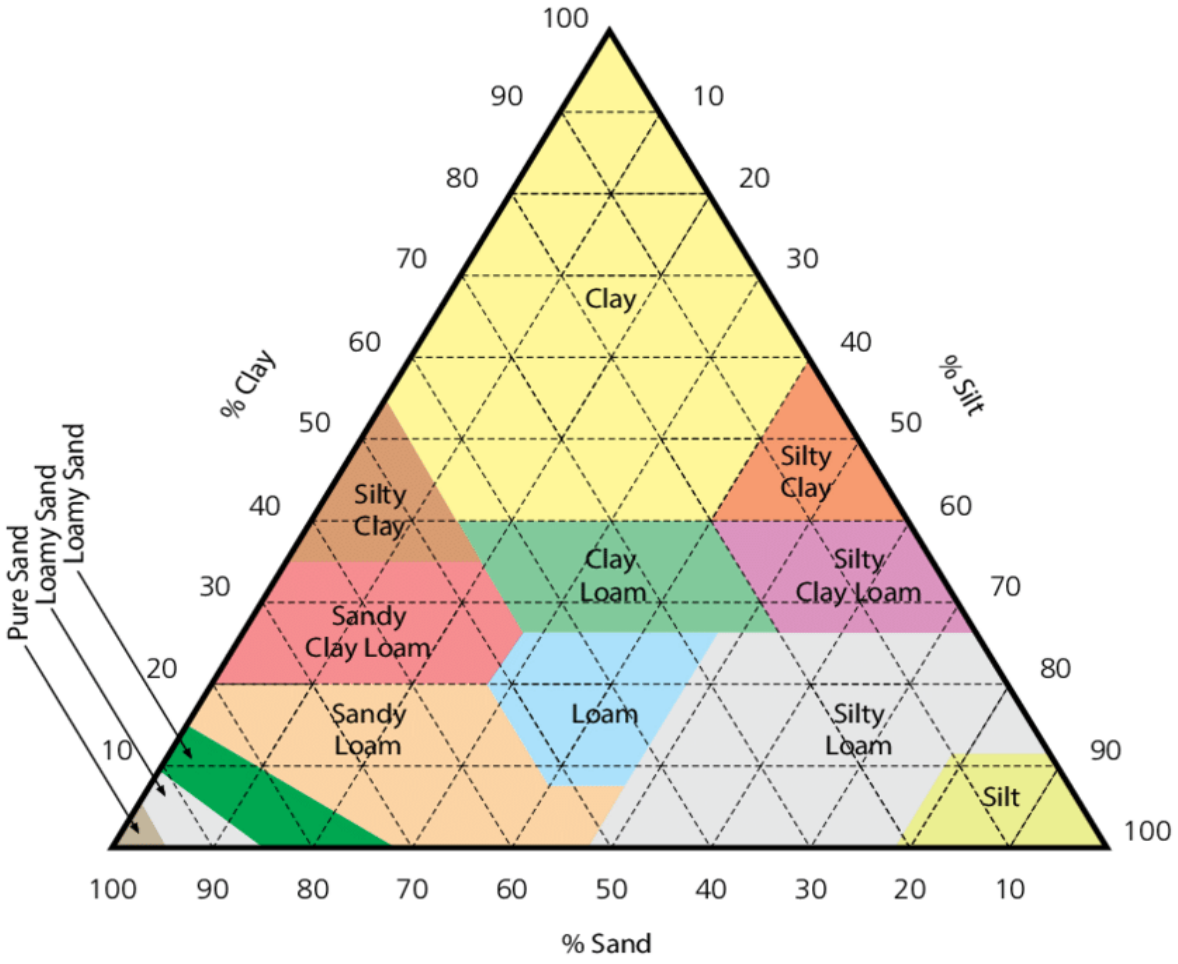


Source: Researchgate

In our soil,

| | |
|---|---|
| % Gravel | 0.40% |
| % of Sand | 49.70% |
| % of Silt | 40.60% |
| % of Clay | 9.30% |

So the soil is classified as loam according to Textural classification

## B-2 AASHTO classification of Soil:

| General classification | Granular materials (35% or less of total sample passing No. 200) | | | | | | |
|---|---|---|---|---|---|---|---|
| | A-1 | | | A-2 | | | |
| Group classification | A-1-a | A-1-b | A-3 | A-2-4 | A-2-5 | A-2-6 | A-2-7 |
| Sieve analysis (percentage passing) | | | | | | | |
| No. 10 | 50 max. | | | | | | |
| No. 40 | 30 max. | 50 max. | 51 min. | | | | |
| No. 200 | 15 max. | 25 max. | 10 max. | 35 max. | 35 max. | 35 max. | 35 max. |
| Characteristics of fraction passing No. 40 | | | | | | | |
| Liquid limit | | | | 40 max. | 41 min. | 40 max. | 41 min. |
| Plasticity index | 6 max. | | NP | 10 max. | 10 max. | 11 min. | 11 min. |
| Usual types of significant constituent materials | Stone fragments, gravel, and sand | | Fine sand | Silty or clayey gravel and sand | | | |
| General subgrade rating | Excellent to good | | | | | | |

| General classification | Silt-clay materials (more than 35% of total sample passing No. 200) | | | |
|---|---|---|---|---|
| Group classification | A-4 | A-5 | A-6 | A-7<br>A-7-5[a]<br>A-7-6[b] |
| Sieve analysis (percentage passing) | | | | |
| No. 10 | | | | |
| No. 40 | | | | |
| No. 200 | 36 min. | 36 min. | 36 min. | 36 min. |
| Characteristics of fraction passing No. 40 | | | | |
| Liquid limit | 40 max. | 41 min. | 40 max. | 41 min. |
| Plasticity index | 10 max. | 10 max. | 11 min. | 11 min. |
| Usual types of significant constituent materials | Silty soils | | Clayey soils | |
| General subgrade rating | Fair to poor | | | |

[a]For A-7-5, $PI \leq LL - 30$
[b]For A-7-6, $PI > LL - 30$

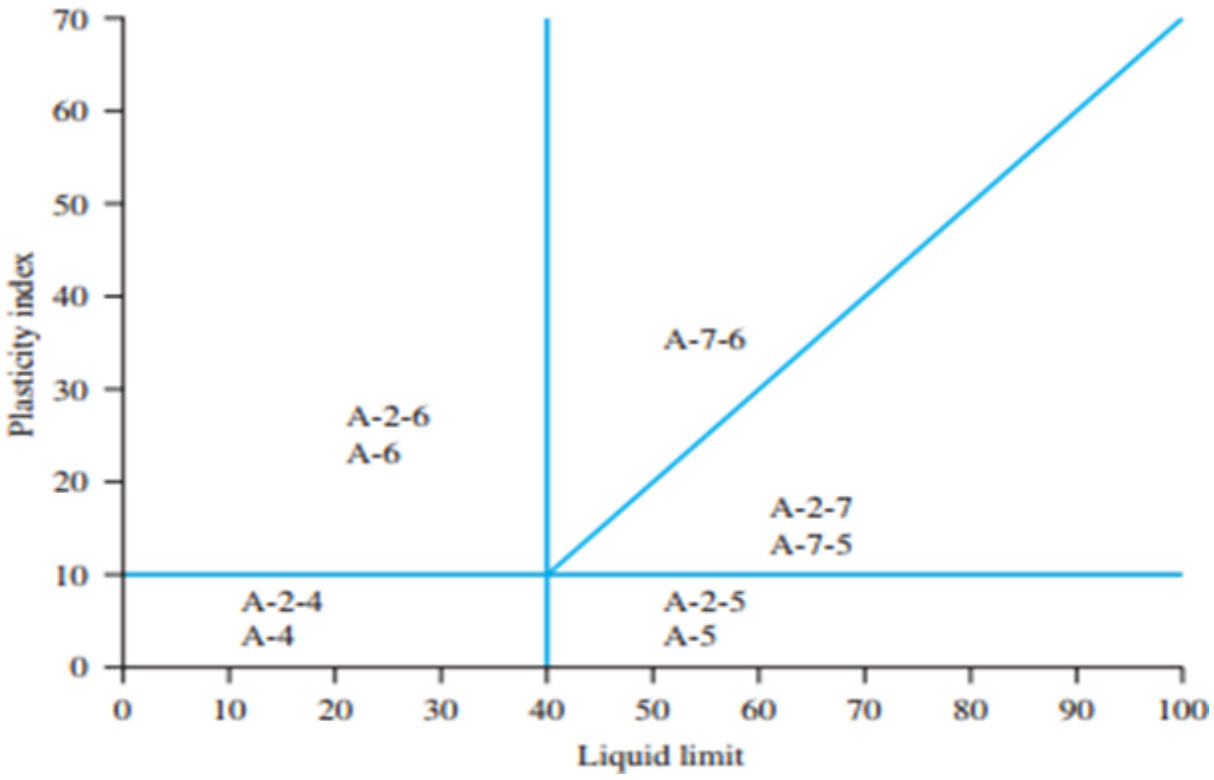


Source: Bajra M Das

Group index is calculated as:

$GI = (F_{200} - 35)[0.2 + 0.05(LL - 40)] + 0.01(F_{200} - 15)(PI - 10)$

In our soil,

$F_{200}$ =79.41%

Average liquid limit=36.328%

Average plastic limit=29.214%

Plasticity Index=7.114

So, soil is classified as A-4(0)

**3.Unified classification of Soil**

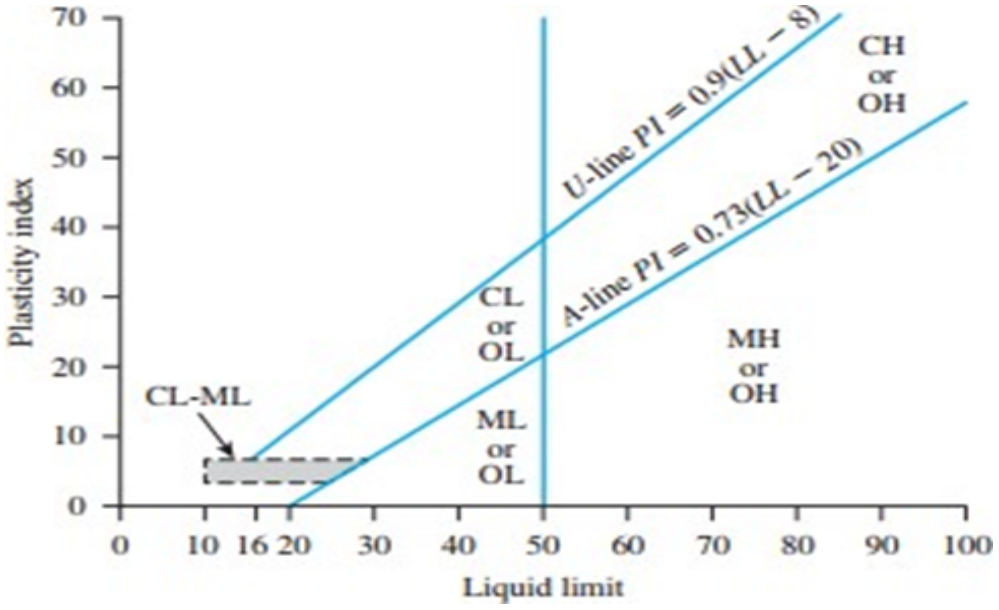


Source: Bajra M Das

In our soil,

$F_{200}$ =79.41%

Average liquid limit=36.328%

Average plastic limit=29.214%

Plasticity Index=7.114

So, according to Unified classification, the soil is classified as ML

i.e Low plasticity inorganic silt

# APPENDIX-C

## Analytical Calculations for Design and Validation of CPRF

**C-1: Load capacity of single pile**

| | | |
|---|---|---|
| Length of Pile | 15m | |
| Diameter of Pile | 1m | |
| Cohesion of soil | 13.857 | |
| Nc | 21.6 | |
| Nq | 11.345 | |
| Nr | 11.836 | |
| α | 0.95 | |
| σ' | 124.29 kN/m2 | |
| k | 0.568 | |
| tanδ | 0.4786 | |
| Skin resistance | αCAs+kσ'vtanδAs | 1416.45 kN |
| Base Resistance | cNc + σ' Nq + 0.5ϒBNϒ | 1814.6 kN |
| Total capacity of single pile | 3231.05 kN | |

**C-2: Group efficiency calculation**

| Efficiency Calculation | No. of Piles | θ= tan-1(d/s) | E |
|---|---|---|---|
| $\eta$ = 1-θ((n-1)m+(m-1)n)/90mn | 9*9 | 14.036 | 72.27% |

**C-3: Pile group capacity calculation**

| Pile length | Efficiency | Number of pile | Ultimate capacity of single pile | Ultimate capacity of Group pile |
|---|---|---|---|---|
| | | | kN | kN |
| 15 m | 72.27% | 81 | 3231.05 | 189141.47 |
| Total pile group capacity in kN | | | | 189141.47 |

**C-4: Raft bearing capacity calculation**

| | | |
|---|---|---|
| Thickness of raft | T | 0.6m |
| Depth of raft from surface | Df | 2.5m |
| Shear strength parameter | C | 13.857 |
| ϕ | 25.58 | |
| Bearing capacity factors | | |
| Nc | 21.6 | |
| Nq | 11.345 | |
| Nr | 11.836 | |
| Unit Weight of soil at depth of raft | 17.45 | |
| Shape Factor | | |
| Fcs=1+(B/L)(Nq/Nc) | 1.525 | |
| Fqs=1+(B/L)tanϕ | 1.479 | |
| Frs=1-0.4(B/L) | 0.6 | |
| Depth factor | | |
| Fcd=Fqd-(1-Fqd)/(Nctanϕ) | 1.002 | |
| Fqd=1+2tanϕ(1- sinϕ)2(Df/B) | 1.021 | |

| | | |
|---|---|---|
| Frd=1 | 1 | |
| Ultimate capacity of raft in kN/m2 | qu=cNcFcsFcd+q(Nq-1)Fqs Fqd+0.5ɣBNrFrsFrd | 608.79 kN/m2 |

**C-5: Calculation of interaction factors**

| | |
|---|---|
| Settlement of pile raft foundation(w) | 0.05827 |
| Width of raft(Br) | 36 |
| Diameter of pile(Dp) | 1 |
| Average Spacing of pile(S) | 4 |
| Pile-Pile interaction factor(αpp) | 72.27 |
| Pile-Raft interaction factor(αpr) | |
| αpr=Qp-CPRF/Qgroup piles=1-exp(-10.55(w/Br)$^{0.26}$) | 0.7862 |
| Raft-Pile interaction factor(αrp) | |
| η=3.5(w/Br)-0.06(S/Dp)-0.51Dp+1.27 | 0.5256 |
| αrp=$Q_{R\text{-}CPRF}$/Qunpiled raft=η+(η-αpr)*$Q_{PG}/Q_{UR}$ | 0.539 |

**C-6: Calculation of Bearing Capacity and Factor of Safety**

| | |
|---|---|
| Ultimate load Capacity of Raft (Qraft) | 788991.84kN |
| Pile-Pile interaction factor (αpp) | 0.7227 |
| Ultimate load Capacity of Pile with pile- pile interaction factor (Qpile) | 189141.47kN |
| Pile-Raft interaction factor (αpr) | 0.7862 |
| Raft-Pile interaction factor(αrp) | 0.539 |
| Bearing Capacity of CPRF (Qu=Qraft*αrp+ Qpile*αpr) | 573969.62kN |
| Total Structural load (P) | 129600 kN |
| Factor of Safety of structure (FOS=Qu/P) | 4.42 |

**C-7: Stiffness of single Pile**

| | |
|---|---|
| Diameter of pile(d) in | 1m |
| Pile length in m | 15m |
| Gs of soil in $kN/m^2$ | 2261.255 |
| Gs at pile base in kN/m2 | 2261.255 |
| Poisson Ratio | 0.2 |
| Ratio of Average Gs to Gs at base (ρ) | 1 |
| ζ = In [5ρ(1-ν)*L/d] | 4.008 |
| Stiffness of Single pile(Kp), kN/m | 51867.84 |

Here,kp= Pt/wt =dGL*(2dbGb/(1-v)dGL) + 2**π**/ζ*(Gavg/ GL)*( L/ d)

**C-8: Stiffness of group of Pile**

| | |
|---|---|
| Efficiency Component pile(e) | 0.55(0.5-0.6) |
| Stiffness of Group pile(Kg): $Kg= n^{1-e}$ Kp | |
| Average stiffness of a group pile as a group action of 81 Nos of 15 m piles in kN/m | 374728.19 |

**C-9: Stiffness of Raft**

| | |
|---|---|
| Length of the section in the bending axis(B) | 36 |
| Gs at raft base in kN/m2 | 2261.255 |
| Raft Stiffness(Kr) in kN/m=2.25GB/(1-v) | 228952.1 |

**C-10: Stiffness of Piled Raft**

| | |
|---|---|
| $\alpha_{rp}$ | 0.539 |
| Kp | 374728.19 |
| Kr | 228952.1 |
| Kpr | 433886.01 |

Here, $K_{pr} = (K_p+K_r(1-2\alpha_{rp}))/( 1-\alpha_{rp}^2(K_r/K_p))$

**C-11: Settlement of Piled Raft**

| | |
|---|---|
| Settlement of the raft without pile under total load(Se) (from Plaxis) | 0.1171 |
| Raft stiffness (Kr) | 228952.1 |
| Pile Raft Stiffness(Kpr) | 433886.01 |
| Pile Raft Settlement(Spr)=Kr*Se/Kpr | 61.78mm |

**C-12: Load Sharing**

| | | |
|---|---|---|
| Stiffness of group Pile (Kp) | | 374728.2 |
| Stiffness of Raft(Kr) | | 228952.1 |
| Load taken by raft to pile,<br>X = Pr / Pt = Pr / (Pr + Pp) =(1-αrp)Kr / (Kp + (1-2αrp)Kr) | | 0.2958 |
| Total Structural load in kN | | 129600 |
| Load taken by pile | 70.43% | 91269.84 |
| Load taken by raft | 29.57% | 38330.16 |

# APPENDIX-D

## Table of Bearing Capacity Factors

Bearing capacity factors for Meyerhoff equation:

| $\phi'$ | $N_c$ | $N_q$ | $N_\gamma$ | $\phi'$ | $N_c$ | $N_q$ | $N_\gamma$ |
|---|---|---|---|---|---|---|---|
| 0 | 5.14 | 1.00 | 0.00 | 26 | 22.25 | 11.85 | 12.54 |
| 1 | 5.38 | 1.09 | 0.07 | 27 | 23.94 | 13.20 | 14.47 |
| 2 | 5.63 | 1.20 | 0.15 | 28 | 25.80 | 14.72 | 16.72 |
| 3 | 5.90 | 1.31 | 0.24 | 29 | 27.86 | 16.44 | 19.34 |
| 4 | 6.19 | 1.43 | 0.34 | 30 | 30.14 | 18.40 | 22.40 |
| 5 | 6.49 | 1.57 | 0.45 | 31 | 32.67 | 20.63 | 25.99 |
| 6 | 6.81 | 1.72 | 0.57 | 32 | 35.49 | 23.18 | 30.22 |
| 7 | 7.16 | 1.88 | 0.71 | 33 | 38.64 | 26.09 | 35.19 |
| 8 | 7.53 | 2.06 | 0.86 | 34 | 42.16 | 29.44 | 41.06 |
| 9 | 7.92 | 2.25 | 1.03 | 35 | 46.12 | 33.30 | 48.03 |
| 10 | 8.35 | 2.47 | 1.22 | 36 | 50.59 | 37.75 | 56.31 |
| 11 | 8.80 | 2.71 | 1.44 | 37 | 55.63 | 42.92 | 66.19 |
| 12 | 9.28 | 2.97 | 1.69 | 38 | 61.35 | 48.93 | 78.03 |
| 13 | 9.81 | 3.26 | 1.97 | 39 | 67.87 | 55.96 | 92.25 |
| 14 | 10.37 | 3.59 | 2.29 | 40 | 75.31 | 64.20 | 109.41 |
| 15 | 10.98 | 3.94 | 2.65 | 41 | 83.86 | 73.90 | 130.22 |
| 16 | 11.63 | 4.34 | 3.06 | 42 | 93.71 | 85.38 | 155.55 |
| 17 | 12.34 | 4.77 | 3.53 | 43 | 105.11 | 99.02 | 186.54 |
| 18 | 13.10 | 5.26 | 4.07 | 44 | 118.37 | 115.31 | 224.64 |
| 19 | 13.93 | 5.80 | 4.68 | 45 | 133.88 | 134.88 | 271.76 |
| 20 | 14.83 | 6.40 | 5.39 | 46 | 152.10 | 158.51 | 330.35 |
| 21 | 15.82 | 7.07 | 6.20 | 47 | 173.64 | 187.21 | 403.67 |
| 22 | 16.88 | 7.82 | 7.13 | 48 | 199.26 | 222.31 | 496.01 |
| 23 | 18.05 | 8.66 | 8.20 | 49 | 229.93 | 265.51 | 613.16 |
| 24 | 19.32 | 9.60 | 9.44 | 50 | 266.89 | 319.07 | 762.89 |
| 25 | 20.72 | 10.66 | 10.88 | | | | |

Source: Bajra M. Das

# APPENDIX-E

## Relation Between Poisson's Ratio and Liquid Limit of Soil

| Type of Soil | Liquid limit $I_L$ | The Poisson's ratio $v$ at a void ratio $e$ equal to | | | |
|---|---|---|---|---|---|
| | | 0.55 | 0.65 | 0.75 | 0.85 |
| Sandy loam | $0 \le I_L \le 0.25$ | 0.2200 | 0.2344 | 0.2556 | – |
| | $0.25 \le I_L \le 0.75$ | 0.2402 | 0.2556 | 0.2784 | 0.3030 |
| Loam | $0 \le I_L \le 0.25$ | 0.2211 | 0.2211 | 0.2424 | 0.2516 |
| | $0.25 \le I_L \le 0.50$ | 0.2332 | 0.2441 | 0.2555 | 0.2745 |
| | $0.50 \le I_L \le 0.75$ | – | 0.2631 | 0.2763 | 0.2955 |
| Clay | $0 \le I_L \le 0.25$ | – | 0.2281 | 0.2386 | 0.2472 |
| | $0.25 \le I_L \le 0.50$ | – | 0.2415 | 0.2498 | 0.2591 |
| | $0.50 \le I_L \le 0.75$ | – | 0.2622 | 0.2700 | 0.2840 |

Source: semanticscholar.org

# APPENDIX-F

## Pile Location Table

**F-1: Pile Location Table**

| SN | Diameter of Pile(m) | Length of Pile(m) | X(m) | Y(m) |
|---|---|---|---|---|
| 1 | 1 | 15 | -16 | 16 |
| 2 | 1 | 15 | -12 | 16 |
| 3 | 1 | 15 | -8 | 16 |
| 4 | 1 | 15 | -4 | 16 |
| 5 | 1 | 15 | 0 | 16 |
| 6 | 1 | 15 | 4 | 16 |
| 7 | 1 | 15 | 8 | 16 |
| 8 | 1 | 15 | 12 | 16 |
| 9 | 1 | 15 | 16 | 16 |
| 10 | 1 | 15 | -16 | 12 |
| 11 | 1 | 15 | -12 | 12 |
| 12 | 1 | 15 | -8 | 12 |
| 13 | 1 | 15 | -4 | 12 |
| 14 | 1 | 15 | 0 | 12 |
| 15 | 1 | 15 | 4 | 12 |
| 16 | 1 | 15 | 8 | 12 |
| 17 | 1 | 15 | 12 | 12 |
| 18 | 1 | 15 | 16 | 12 |
| 19 | 1 | 15 | -16 | 8 |
| 20 | 1 | 15 | -12 | 8 |
| 21 | 1 | 15 | -8 | 8 |
| 22 | 1 | 15 | -4 | 8 |
| 23 | 1 | 15 | 0 | 8 |

| | | | | |
|---|---|---|---|---|
| 24 | 1 | 15 | 4 | 8 |
| 25 | 1 | 15 | 8 | 8 |
| 26 | 1 | 15 | 12 | 8 |
| 27 | 1 | 15 | 16 | 8 |
| 28 | 1 | 15 | -16 | 4 |
| 29 | 1 | 15 | -12 | 4 |
| 30 | 1 | 15 | -8 | 4 |
| 31 | 1 | 15 | -4 | 4 |
| 32 | 1 | 15 | 0 | 4 |
| 33 | 1 | 15 | 4 | 4 |
| 34 | 1 | 15 | 8 | 4 |
| 35 | 1 | 15 | 12 | 4 |
| 36 | 1 | 15 | 16 | 4 |
| 37 | 1 | 15 | -16 | 0 |
| 38 | 1 | 15 | -12 | 0 |
| 39 | 1 | 15 | -8 | 0 |
| 40 | 1 | 15 | -4 | 0 |
| 41 | 1 | 15 | 0 | 0 |
| 42 | 1 | 15 | 4 | 0 |
| 43 | 1 | 15 | 8 | 0 |
| 44 | 1 | 15 | 12 | 0 |
| 45 | 1 | 15 | 16 | 0 |
| 46 | 1 | 15 | -16 | -4 |
| 47 | 1 | 15 | -12 | -4 |
| 48 | 1 | 15 | -8 | -4 |

| | | | | |
|---|---|---|---|---|
| 49 | 1 | 15 | -4 | -4 |
| 50 | 1 | 15 | 0 | -4 |
| 51 | 1 | 15 | 4 | -4 |
| 52 | 1 | 15 | 8 | -4 |
| 53 | 1 | 15 | 12 | -4 |
| 54 | 1 | 15 | 16 | -4 |
| 55 | 1 | 15 | -16 | -8 |
| 56 | 1 | 15 | -12 | -8 |
| 57 | 1 | 15 | -8 | -8 |
| 58 | 1 | 15 | -4 | -8 |
| 59 | 1 | 15 | 0 | -8 |
| 60 | 1 | 15 | 4 | -8 |
| 61 | 1 | 15 | 8 | -8 |
| 62 | 1 | 15 | 12 | -8 |
| 63 | 1 | 15 | 16 | -8 |
| 64 | 1 | 15 | -16 | -12 |
| 65 | 1 | 15 | -12 | -12 |
| 66 | 1 | 15 | -8 | -12 |
| 67 | 1 | 15 | -4 | -12 |
| 68 | 1 | 15 | 0 | -12 |
| 69 | 1 | 15 | 4 | -12 |
| 70 | 1 | 15 | 8 | -12 |
| 71 | 1 | 15 | 12 | -12 |
| 72 | 1 | 15 | 16 | -12 |
| 73 | 1 | 15 | -16 | -16 |

| | | | | |
|---|---|---|---|---|
| 74 | 1 | 15 | -12 | -16 |
| 75 | 1 | 15 | -8 | -16 |
| 76 | 1 | 15 | -4 | -16 |
| 77 | 1 | 15 | 0 | -16 |
| 78 | 1 | 15 | 4 | -16 |
| 79 | 1 | 15 | 8 | -16 |
| 80 | 1 | 15 | 12 | -16 |
| 81 | 1 | 15 | 16 | -16 |

# APPENDIX-G

## Cost Estimation

## G-1: General Quantity Estimation

| SN | Description | No. | Length(m) | Breadth(m) | Height(m) | Quantity | Units | Remarks |
|---|---|---|---|---|---|---|---|---|
| **1** | **Site Clearance** | | | | | | | |
| | Area of light jungle( less than 15 numbers per 100 sq.m) | | 36 | 36 | | 1296 | sq. m | |
| | | | | | | | | |
| **2** | **Earthwork in Excavation** | | | | | | | |
| 1.1 | Raft | 1 | 36 | 36 | 3 | 3888 | cu. m | |
| | **Total** | | | | | 3888 | cu. m | |
| 1.2 | Piles | 81 | | | 15 | 1215 | rm | |
| | **Total** | | | | | **1215** | **rm** | |
| | | | | | | | | |
| | | | | | | | | |
| **3** | **Cement concrete(1:2:4) for RCC works Excluding Reinforcement** | | | | | | | |
| 3.1 | Raft | 1 | 36 | 36 | 0.6 | 777.6 | cu. m | |
| 3.2 | Piles | 81 | Area=3.1416*1*1/4 | | 15 | 954.261 | cu. m | |
| | **Total** | | | | | **1731.861** | **cu. m** | |
| | | | | | | | | |
| **4** | **Steel Reinforcement** | | | | | | | |
| 4.1 | For Raft @1.5% | | 777.6 | | 1.50% | 91.5624 | tonnes | Density of steel= 7850 |

| | | | | | | | | |
|---|---|---|---|---|---|---|---|---|
| | | | | | | | | kg/cu.m |
| 4.2 | For Piles @1.5% | | 954.261 | | 1.50% | 112.3642328 | tonnes | |
| | **Total** | | | | | **203.926** | **tonnes** | |

**G-2: Rate Analysis**

| **Site Clearance** | | | | | | |
|---|---|---|---|---|---|---|
| In area of light jungle (less than 15 number per 100 sqm ) | | | | | | |
| Unit= sq.m (per 10000 sq. m) | | | | | | |
| **SN** | **Name of Item** | **Quantity** | **Unit** | **Rate** | **Amount(NRs.)** | **Remarks** |
| **A** | **Labour** | | | | | |
| | Unskilled | 6 | day | 870 | 5220 | |
| **B** | **Equipment** | | | | | |
| | Excavator | 12 | hour | 3000 | 36000 | |
| | | | | (A+B) | 41220 | |
| C | Contractor overhead and Profit @15% of (A+B) | | | | 6183 | |
| | | | | Grand Total | 47403 | |
| | | | | For 1 sq.m | 4.7403 | |

| | | | | | | |
|---|---|---|---|---|---|---|
| | | | | | | |
| | | **Raft** | | | | |
| **SN** | **Name of Item** | **Quantity** | **Unit** | **Rate** | **Amount(NRs.)** | |
| | **Earthwork in Excavation** | | | | | |
| | **E.W in Excavation** | | | | | |
| A. | Materials | | | Sub Total A | 0 | |
| B. | Labour | | | | | |
| | | | | | | |
| | | | | | | |
| i. | Skilled | 0 | | 1185 | 0 | |
| ii. | Unskilled | 0.7 | day | 870 | 609 | |
| | | | | Sub Total B | 609 | |
| C | Machinery | | | | | |
| | Hire and running charges for Excavator including Diesel | 0.5 | hour | 3000 | 2000 | |
| | Tipper 5.5 cu.m capacity for disposal of muck from excavation Place | 0.3 | hour | 2000 | 600 | |
| | | | | Sub Total C | 2600 | |
| | | | | | | |

| | | | | | | |
|---|---|---|---|---|---|---|
| | | | | | | |
| | | | | Total (A+B+C) | 3209 | |
| D. | Contractors overhead and profit @15% of total | | | | 481.35 | |
| | | | | Grand Total | 3690.35 | |
| | Cost of Excavation Per cu.m | | | | 3690.35 | |
| | | | | | | |
| **Piling** | | | | | | |
| Pile Diameter= 1000 mm | | | | | | |
| Unit= Meter (For 15m depth) | | | | | | |
| **SN** | **Name of Item** | **Quantity** | **Unit** | **Rate** | **Amount(NRs.)** | |
| **A** | **Labour** | | | | | |
| | Skilled | 5 | day | 1185 | 5925 | |
| | Unskilled | 50 | day | 870 | 43500 | |
| | | | | Sub Total A | 49425 | |
| **B** | **Materials** | | | | | |
| | Bentonite | 75 | kg | 40 | 3000 | |
| **C** | **Equipment( for boring and construction )** | | | | | |

| | | | | | | |
|---|---|---|---|---|---|---|
| | Piling rig ( with all accessories) | 9 | hour | 2000 | 18000 | |
| | Crane | 9 | hour | 3000 | 27000 | |
| | Bentonite Pump | 9 | hour | 1000 | 9000 | |
| | | | | Total | 54000 | |
| | | | | **(A+B+C)** | 106425 | |
| D | Contractors overhead and Profit @15% of (A+B+C) | | | | 15963.75 | |
| | | | | **Grand Total** | 122388.75 | |
| | | | | For 1m | 8159.25 | |
| | | | | | | |
| | | | | | | |
| **Providing and laying of Cement Concrete in Foundation** | | | | | | |
| | PCC Grade M 15 | | | | | |
| | Unit= cum (for 15 cum) | | | | | |
| **SN** | **Name of Item** | **Quantity** | **Unit** | **Rate** | **Amount(NRs.)** | |
| **A** | **Labour** | | | | | |
| | Skilled | 3 | day | 1185 | 3555 | |
| | Unskilled | 30 | day | 870 | 26100 | |
| | | | | Sub Total A | 29655 | |

| | | | | | | |
|---|---|---|---|---|---|---|
| **B** | **Materials** | | | | | |
| | Cement | 4.13 | tonnes | 850(per 50 kg) | 70210 | |
| | 20mm aggregate | 4.05 | cu.m | 2780 | 11259 | |
| | Sand | 6.75 | cu.m | 3000 | 20250 | |
| | Water | 2 | kl | 260 | 520 | |
| | | | | Sub Total B | 102239 | |
| C | Equipment | | | | | |
| | Concrete Mixer | 6 | hour | 1000 | 6000 | |
| | Generator | 6 | hour | 1000 | 6000 | |
| | | | | **(A+B+C)** | 143894 | |
| D | Formwork @ 4% of (A+B+C) | | | | 5755.76 | |
| | | | | (A+B+C+D) | 149649.76 | |
| E | Contractor Overhead and Profit @15% of (A+B+C+D) | | | | 22447.464 | |
| | | | | Grand Total | 172097.22 | |
| | | | | For 1 cu.m | 11473.148 | |
| | | | | | | |
| **Providing and laying ,fitting and placing TMT steel reinforcemen** | | | | | | |

| | | | | | | |
|---|---|---|---|---|---|---|
| **t** | | | | | | |
| | Unit= tonne (For 1 tonne) | | | | | |
| **SN** | **Name of Item** | **Quantity** | **Unit** | **Rate** | **Amount(NRs.)** | |
| **A** | **Labour for straightening, cutting, bending, shifting to site, tying and placing in position** | | | | | |
| | Skilled(Black smith) | 4 | days | 1185 | 4740 | |
| | Unskilled | 10 | days | 870 | 8700 | |
| | | | | Sub Total A | 13440 | |
| **B** | **Material** | | | | | |
| | TMT Bars | 1.15 | tonnes | 95000 | 109250 | |
| | Binding Wire | 9 | kg | 100 | 900 | |
| | | | | Sub Total B | 110150 | |
| C | Hire of Tools and Plants @ 3% of unskilled labour | | | | 261 | |
| | | | | (A+B+C) | 123851 | |
| D | Contractor Overhead and Profit @15% of (A+B+C) | | | | 18577.65 | |
| | | | | Grand Total | 142428.65 | |

## G-3: Abstract of Cost

| SN | Description of Work | Unit | Rate | Quantity | Amount(Nrs.) |
|---|---|---|---|---|---|
| 1 | Site Clearance | sq.m | 4.7403 | 1296 | 6143.4288 |
| 2 | Earthwork in Excavation For Raft | cu.m | 3690.35 | 3888 | 14348080.8 |
| 3 | Piling | rm | 8159.25 | 1215 | 9913488.75 |
| 4 | Providing and laying of Cement Concrete in Foundation | | | | |
| | Raft | cu.m | 11473.15 | 777.6 | 8921520.092 |
| | Pile | cu.m | 11473.15 | 954.261 | 10948377.94 |
| | | | | Total | 19869898.03 |
| 5 | Steel Reinforcement | tonnes | 142428.7 | 203.9266328 | 29044995 |
| | Sub Total | | | | 73182606.01 |
| | | | | Add Contingencies= 4% | 2927304.24 |
| | | | | **Grand Total** | 76109910.25 |